Port-based teleportation of continuous quantum variables

by

Jason Boisselle

A thesis

presented to the university of Waterloo

in fulfilment of the

thesis requirement for the degree of

Master of Mathematics

in

Applied Mathematics

Waterloo, Ontario, Canada, 2014

I hereby declare that I am the sole author of this thesis. This is a true copy of the thesis, including any required final revisions, as accepted by my examiners.

I understand that my thesis may be made electronically available to the public.

Abstract

Quantum teleportation allows to transmit quantum information using classical information and entanglement only. Port-based teleportation is a variation of this procedure that involves simpler recovery operations to obtain the transmitted quantum information. This provides significant advantages in different applications such as instantaneous non-local computation.

We study port-based teleportation for continuous variable systems. We connect this problem to hypothesis testing, generalizing a result already known for finite-dimensional systems. Similarly, we present a relation between entanglement fidelity and average fidelity valid for both finite and infinite-dimensional systems. Finally, we present a protocol that reduces port-based teleportation for infinite-dimensional systems to port-based teleportation of finite-dimensional systems which allows us to show that the former task is, at least in principle, possible with a finite amount of resources.

Acknowledgement

I first want to thank my supervisor Robert Koenig for his infinite patience. Without his advice, none of this would have been possible.

I would like to also thank my family and friends, both back home and the ones I made in Waterloo, who made this whole experience easier.

Finally, I want to specially thank my uncle Gilles because he has always been an example for me, even when I did not realize it.

Contents

List of Figures

1   Introduction

Quantum teleportation might be one of the most iconic features of quantum information. It allows two people to perform quantum communication by sharing entanglement and using classical communication. Apart from its obvious importance for potential quantum communication, quantum teleportation figures prominently in quantum key distribution and quantum computing. This justifies the interest of many researchers in this topic. As a consequence, several variations of the original protocol have been developed.

One of the variations of the standard quantum teleportation scheme is port-based teleportation [18, 19]. It has the advantage of greatly simplifying the post-processing required at the end of the protocol. The asymmetry between the operations the two communicating parties need to do is important. The sender must be able to perform measurements on quantum systems while the receiver only needs to be able to discard quantum systems according to the classical information he receives. No other correction operation is required and he obtains a high-fidelity approximation to the input state. Therefore, it is easier to apply quantum operations on the teleported state, even if the classical information as not yet reached the receiver.

Applications involving quantum teleportation benefit greatly from the operational asymmetry between the sender and the receiver. One of these applications is instantaneous non-local computations. Two people are given half of a bipartite state each and their goal is to apply a non-local unitary on their bipartite state using only one round of classical communication, local operations and entanglement. Vaidman [31] explained how to accomplish this task by using standard quantum teleportation, but his procedure required an amount of entanglement doubly exponential in the number of qubits of the bipartite state. This task can be done more efficiently using port-based teleportation. Indeed, Beigi and Koenig [17] showed that doing so would reduce the consumption of entanglement by an exponential amount.

Another interesting application is the universal programmable processor, a scheme proposed by

Ishizaka and Hiroshima [19], the inventors of port-based teleportation. The idea is that it is possible to store a quantum operation on the resource state and when performing teleportation, the quantum operation will be applied automatically to the output state. Using standard quantum teleportation gives a probabilistic processor with probability of success $\frac{1}{4}$ for a single qubit. Intuitively, this is because the correction operation the receiver needs to apply will not in general commute with the quantum operation that needs to be applied on the input state. Port-based teleportation however does not have this problem [19] since the correction operation only involves choosing the right port and discarding the rest. Because of this, port-based teleportation is more suited to this application than the standard teleportation.

The first proofs of principle showing the potential power of quantum computing used finite-dimensional systems because they are easier to handle mathematically than their infinite-dimensional counterparts. Quantum key distribution [10], quantum teleportation [11] and Shor's factorization algorithm [12] were all first designed with finite-dimensional states in mind. The study of quantum information is now in a phase where researches are trying to implement these algorithms in experiments. However, finite-dimensional systems that were convenient to use in abstract proofs are not necessarily the easiest systems to use in a laboratory. It is for this reason that one of the variations of quantum teleportation was proposed for continuous variable systems. This was first shown by Vaidman [25] and later on it was refined by Braunstein and Kimble [26].

Port-based teleportation relies on finite-dimensional systems and its fidelity depends explicitly on the dimension of the state that is teleported. At first sight, it might seem like it would require an infinite amount of entanglement to teleport continuous variable systems. In this thesis, we will investigate the possibility of using port-based teleportation for infinite-dimensional systems. More precisely, we will specialize our treatment to Gaussian states [28, 29]. Gaussian states are useful because, even though they are states on infinite-dimensional systems, they can be compactly described by their first and second moments. This greatly facilitate their manipulation in calculations. Furthermore, Gaussian states arise naturally in quantum optics. For this reason, we would like to

learn whether it is possible to implement port-based teleportation with basic tools of quantum optics. In this spirit, we will mainly talk about coherent states as our states to teleport because they are easily generated with lasers and two-mode squeezed states as our entanglement resource since they are ubiquitous in the description of entanglement in quantum optics.

The search for a good measurement to implement port-based teleportation can be rephrased in terms of a certain quantum hypothesis problem, a fact that was previously observed [19] in the finite-dimensional case. One of our main result is to provide a more general relation between the fidelity of the teleportation process and a distinguishability problem. In the special case of finite-dimensional systems, this allows us to recover the known relation. In the case of squeezed state resources and teleportation of coherent states, we obtain a hypothesis testing problem involving an ensemble of Gaussian states. Unfortunately, there are presently no good bounds for this problem, but this specific case is at least easier to state and analyse. On a more conceptual level, we use the relationship between fidelity and distinguishing success probability to relate port-based teleportation to superdense coding. We find that port-based teleportation is equivalent to a port-based version of the latter.

Finally, we consider a slightly different problem, where we relax the asymmetric requirements for sender and receiver. We construct a protocol that provides a proof of principle of the possibility of doing port-based teleportation in the infinite-dimensional case. However, it requires pre- and post-processing by both parties. This protocol is constructed by reduction to the finite-dimensional protocol. However, it does not rely solely on linear quantum optics components; finding (or even showing existence of) such a realization is an open problem.

Outline

This document is organized as follow. Chapter 2 presents the basic concepts used in quantum information (Section 2.1) and in the task of distinguishing a given ensemble of quantum states (Section

3

2.2). Chapter 3 gives an introduction to continuous variable systems, starting with the quantization of electrical fields (Section 3.1) before giving various examples of one-mode states (Section 3.2). It subsequently presents concepts such as Gaussian states (Section 3.3) and Gaussian operations (Section 3.4) before giving an overview of entanglement (Section 3.5) in this specific context. Chapter 4 presents a reminder of teleportation both for finite-dimensional and infinite-dimensional systems (Section 4.1 and Section 4.2) before focusing on the teleportation of coherent states (Section 4.3) and the benchmarks to assess the quality of teleportation (Section 4.4). Chapter 5 focuses on port-based teleportation (Section 5.1) and the relation it has to a quantum hypothesis problem (Section 5.2) before giving appropriate lower bounds for its fidelity (Section 5.3) and exploring the qubit case (Section 5.4). Afterwards, we discuss different applications of port-based teleportation (Section 5.5) and the related superdense coding scheme associated with port-based teleportation (Section 5.6). Chapter 6 presents most of our findings on port-based teleportation for continuous variables such as the appropriate figure of merit (Section 6.1), the relation between entanglement fidelity and average fidelity (Section 6.2) and more importantly, a protocol that provides an idea of the resources necessary to do port-based teleportation with coherent states (Section 6.3). The appendices provide complete calculations of some points that were not essential to the main text.

2 Preliminaries

This section is a presentation of basic tools that will be used throughout this document. For a more complete review of quantum information, we recommend [1].

2.1 Quantum information concepts

Here we provide a brief introduction to basic concepts of quantum information. For more detailed information, we refer the reader to the literature (see e.g. [1] and the introduction of [27]).

2.1.1 Quantum states

A quantum state is described by its density operator ρ which satisfies the following properties

1. $\text{tr}(\rho) = 1$ (normalization)

2. $\rho = \rho^\dagger$ (Hermitian)

3. $\rho > 0$ (positive).

Density matrices are more general than pure states because they contain the fundamental uncertainty due to quantum mechanics as well as the uncertainty due to the lack of access to part of a system. In this regard, the density matrix of a quantum state contains all the information available to an observer doing measurements on this quantum state.

One way to illustrate this lack of information is to use the partial trace. Assume someone, say Alice, prepared a quantum state on systems A and B. Alice has complete knowledge of the state ρ_{AB}. Now suppose Alice sends the B system to another person, say Bob. He does not know how the state was generated so the density matrix of his quantum state, from his perspective, is given by the partial trace of ρ_{AB}

$$\rho_B = \text{tr}_A(\rho_{AB}).$$

After sending system B, Alice does not know anymore what is happening with system B. From her point of view, it is equivalent to discarding system B. The quantum state she has in her possession is also described using the partial trace

$$\rho_A = \text{tr}_B(\rho_{AB}).$$

One note on the "church of the larger Hilbert space" [2], it is always possible to represent a density matrix as being the result of discarding a subsystem of a pure state on a larger Hilbert

space

$$\rho_A = \mathsf{tr}_B(|\psi\rangle\langle\psi|_{AB}).$$

It can be argued whether it is physically always possible to embed one system into a larger one if the universe is finite, but mathematically this concept is well defined and often useful.

2.1.2 Quantum operations

The most general operations $\rho \to \mathcal{E}(\rho)$ that can be applied to quantum states are Completely Positive Trace Preserving maps (CPTP maps for short). This is because such operators should map quantum states to quantum states and therefore preserve unit trace and positivity. A popular way to represent them is by Kraus operators: for every quantum operation $\rho \to \mathcal{E}(\rho)$, there are operators $\{A_i\}$ such that

$$\mathcal{E}(\rho) = \sum_i A_i \rho A_i^\dagger \tag{1}$$

where $\sum_i A_i^\dagger A_i = \mathbb{1}$. Another useful point of view is given by Stinespring's dilation theorem [3]. It relates CPTP maps to unitary transformations by saying that every such map can be seen as adding an ancilla in state ρ_B to a quantum state before applying a unitary U_{AB} and then tracing the ancilla

$$\mathcal{E}(\rho_A) = \mathsf{tr}_B(U_{AB}(\rho_A \otimes \rho_B)U_{AB}^\dagger).$$

In this thesis we will often consider different measurements we can perform on a quantum state. Measurements give an operational meaning to quantum systems as they describe how we interact and collect information from them. The simplest measurement is the von Neumann measurement.

It assumes that for every physical observable there is an operator $\mathcal{O}$ with spectral representation $\mathcal{O} = \sum_i o_i |i\rangle\langle i|$. The characteristics of the measurement are the following

1. Each possible result of the measurement yields the outcome o_i and after the measurement, the system is in the quantum state $|i\rangle$.

2. The probability of measurement outcome o_i is given by $p_i = \langle i|\rho|i\rangle$.

3. If we perform a measurement without checking the result, the density matrix of the quantum state we have is given by $\rho = \sum_i p_i |i\rangle\langle i|$.

Projective measurements are conceptually simple, but they are not the most general measurements we can perform on a quantum system. There is an analogous theorem for measurements to Stinespring's dilation theorem for quantum maps. Neumark's theorem [4] states that the most general measurement one can apply can be seen as the result of adding an ancilla system to the quantum state we want to measure, then applying a von Neumann measurement and discarding the ancilla. The resulting operation is what we call a Positive Operator Valued Measure (POVM for short). It is described by a set of operators $\{E_i\}_{i=1}^N$ satisfying

1. Each operator is positive $E_i \geq 0$ and they sum to the identity $\sum_i E_i = \mathbb{1}$.

2. We have one operator E_i for every outcome i of the measurement.

3. Each outcome i occurs with probability $p_i = \mathsf{tr}(E_i\rho)$ and the normalized post-measurement state is given by

$$\rho_i = \frac{\sqrt{E_i}\rho\sqrt{E_i}^\dagger}{\mathsf{tr}(E_i\rho)}.$$

4. Should we make a measurement without looking at the result, we would then have the state

$$\rho' = \sum_i \sqrt{E_i}\rho\sqrt{E_i}^\dagger. \tag{2}$$

As one can see, the form of (2) is a quantum map (1) with Kraus operators $A_i = \sqrt{E_i}$.

So far, we discussed the case of a finite number of measurement outcomes. If we expect a continuum of values for a measurement, the properties we showed earlier are still valid if they are adapted to continuous variables. For instance, if we have the positive operators $\{E_\alpha\}_\alpha$[1] with measure $d\alpha$, then equation (2) would read

$$\rho' = \int d\alpha \sqrt{E_\alpha}\rho\sqrt{E_\alpha}^\dagger.$$

2.1.3 Fidelities and norms

The fidelity $F(\rho, \sigma)$ of two quantum states ρ, σ is defined as

$$F(\rho, \sigma) = \left[\mathrm{tr}\left(\sqrt{\sqrt{\sigma}\rho\sqrt{\sigma}}\right)\right]^2 \tag{3}$$

and it is symmetric in its inputs [2]. The fidelity is a measure of the closeness of two quantum states, it is 1 if and only if the two states are identical and it is 0 if and only if they have orthogonal

---

[1]Sometimes we will want to identify the system on which the measurement will be applied. In these cases, the system will always be identified by a subscript and the other index will be put in superscript. For instance, E_A^α is the POVM element E_α acting on system A.

[2]This is not obvious from (3). The proof follows from Uhlmann's theorem, see below.

8

supports. For most of our purposes, one of the two inputs will be a pure state, in which case

$$
\begin{aligned}
F(\rho, |\psi\rangle\langle\psi|) &= \text{tr}(\sqrt{|\psi\rangle\langle\psi|\rho|\psi\rangle\langle\psi|})^2 \\
&= \text{tr}(\sqrt{\langle\psi|\rho|\psi\rangle}\sqrt{|\psi\rangle\langle\psi|})^2 \\
&= \langle\psi|\rho|\psi\rangle
\end{aligned}
\tag{4}
$$

because the square root of any projector is the projector itself. If $\rho = |\phi\rangle\langle\phi|$ is also a pure state, the fidelity is the probability of obtaining outcome $|\psi\rangle$ when we measure state $|\phi\rangle$ with any measurement involving the operator $|\psi\rangle\langle\psi|$ in its Kraus decomposition. In other words, it is the overlap between the two states. In general, we have an analogous interpretation given by Uhlmann's theorem [5] which states that

$$
F(\rho, \sigma) = \max_{|\psi\rangle, |\phi\rangle} |\langle\phi|\psi\rangle|^2
$$

where $|\psi\rangle$ and $|\phi\rangle$ are purifications of ρ and σ. This means that the fidelity is the maximum overlap between all possible purifications of the two inputs. Another equivalent formulation is

$$
\sqrt{F(\rho, \sigma)} = \min_{\{E_i\}} \sum_i \sqrt{\text{tr}(\rho E_i)\text{tr}(\sigma E_i)}
$$

where the minimum is over all POVMs $\{E_i\}$. This is related to the optimal POVM an experimentalist can use to distinguish two quantum states. It provides a relation between the quantum measurements one can apply to quantum states and the classical probability distribution that results from the measurements.

We can lift this measure to channels. Consider two arbitrary channels $\mathcal{E}_1$ and $\mathcal{E}_2$. The average

9

fidelity between these two channels is defined as

$$\bar{F}(\mathcal{E}_1, \mathcal{E}_2) = \int F(\mathcal{E}_1(|\psi\rangle\langle\psi|), \mathcal{E}_2(|\psi\rangle\langle\psi|))d\psi$$

where $d\psi$ is the Haar measure on the set of states $|\psi\rangle$. For a teleportation map, we desire that the state at the output will be as close as possible to the input, so usually we will compute $\bar{F}(\mathcal{E}, \mathbb{I})$, i.e. we will compare $\mathcal{E}$ to the identity channel $\mathbb{I}$.

Another measure of the distance of two channels is the entanglement fidelity which measures how close a channel $\mathcal{E}$ is to the identity channel. This measure quantifies how well entanglement is preserved when a quantum channel is applied to one side of a maximally entangled state. Its expression is

$$F_{ent}(\mathcal{E}, |\Phi_d^+\rangle) = F((\mathbb{I} \otimes \mathcal{E})(|\Phi_d^+\rangle\langle\Phi_d^+|), |\Phi_d^+\rangle\langle\Phi_d^+|)$$

where $|\Phi_d^+\rangle = \frac{1}{\sqrt{d}}\sum_i |i\rangle|i\rangle$ for some orthonormal basis $\{|i\rangle\}$ and d is the input dimension. The fidelity is not a metric since $F(\rho, \rho) \neq 0$, but it can still be related to other norms to produce interesting identities. One of these norms is the trace norm $\|\cdot\|_1$, defined as

$$\|\rho\|_1 = \mathsf{tr}\sqrt{\rho^\dagger\rho} = \mathsf{tr}|\rho|.$$

Its interpretation will be discussed later in Section 2.2.1. What is of interest to us for the moment is that the trace distance of two quantum states ρ and σ can be bounded by expressions involving the fidelity [1],

$$1 - \sqrt{F(\rho, \sigma)} \leq \|\rho - \sigma\|_1 \leq \sqrt{1 - F(\rho, \sigma)}. \tag{5}$$

The trace norm induces a norm for superoperators $\mathcal{E}$

$$\|\mathcal{E}\|_1 = \max_{\rho:\|\rho\|_1 \leq 1} \|\mathcal{E}(\rho)\|_1$$

and this further allows us to identify what we call the diamond norm $\| \cdot \|_\diamond$

$$\|\mathcal{E}\|_\diamond = \sup_{k \geq 1} \|\mathcal{E} \otimes \mathbb{I}_{\mathcal{B}(\mathbb{C}^k)}\|_1. \tag{6}$$

This norm finds its relevance in the following interpretation. Given two CPTP maps $\mathcal{E}_1$ and $\mathcal{E}_2$, the quantity

$$\frac{1}{2} + \frac{1}{4}\|\mathcal{E}_1 - \mathcal{E}_2\|_\diamond \tag{7}$$

is the probability of distinguishing the two channels when given one use of either of them with equal probability. The diamond norm can be related to the entanglement fidelity by (as shown in [17])

$$\|\mathcal{E} - \mathbb{I}\|_\diamond \leq 4d\sqrt{1 - F_{ent}(\mathcal{E}, |\Phi_d^+\rangle)} \tag{8}$$

where d is the dimension of the maximally entangled state, $|\Phi_d^+\rangle \in \mathbb{C}^d \otimes \mathbb{C}^d$. One can see that if the entanglement fidelity is close to 1, the diamond norm will become close to 0.

2.2 Distinguishing quantum states

The multiple hypothesis testing problem is the following task: we have to correctly identify one state from the ensemble $\{p_i, \rho_i\}$ using a given POVM $\{E_j\}$. The average probability of success is easy to represent. It is given by the prior probability p_i of being given the state ρ_i multiplied by

the probability of obtaining outcome i (given that ρ_i is measured),

$$p_{succ} = \sum_i p_i \mathsf{tr}(E_i \rho_i).$$

We can try to find the optimal probability of success $p_{succ}^{optimal}$ given by an optimal POVM, i.e. the one that maximizes this expression. This optimization over POVMs is in general non-trivial, so we will discuss a few techniques to study this problem.

2.2.1   Helstrom measurement

Let us first consider the simplest distinguishing task we can think of. We are given either state ρ_0 or state ρ_1, each with probability one half and our task is to find a measurement to maximize our (average) probability of correctly identifying the quantum state given to us. Helstrom investigated this question [6] and had the following reasoning. Consider a POVM $\{E, \mathbb{1} - E\}$, then the probability of success is

$$\begin{aligned} p_{succ} &= \frac{1}{2}\mathsf{tr}(E\rho_0) + \frac{1}{2}(1 - \mathsf{tr}(E\rho_1)) \\ &= \frac{1}{2}(1 + \mathsf{tr}((\rho_0 - \rho_1)E)). \end{aligned}$$

Then it is obvious that we want to maximize $\mathsf{tr}((\rho_0 - \rho_1)E)$ to maximize the probability of success. Since the trace is the sum of the eigenvalues of an operator and $E \leq \mathbb{1}$, the optimal strategy consists in projecting the state onto its eigenspace of positive eigenvalues only. Also, because $\mathsf{tr}(\rho_0 - \rho_1) = 0$, the sum of the positive eigenvalues is minus the sum of the negative eigenvalues, therefore

$$p_{succ} = \frac{1}{2} + \frac{1}{4}\mathsf{tr}|\rho_0 - \rho_1|.$$

The second term is related to the trace distance so we have $p_{succ} = \frac{1}{2} + \frac{1}{4}\|\rho_0 - \rho_1\|_1$. This is analogous to the relation (7) we had for the diamond norm.

2.2.2 Pretty good measurement

The pretty good measurement [7] (abbreviated PGM), as its name suggests, is a measurement that will perform fairly well[3] in many cases. It is especially suitable when the states to distinguish are almost orthogonal. If we have N states to distinguish with uniform prior, the POVM elements for the pretty good measurement read

$$E_i = \left(\sum_{j=1}^{N} \rho_j\right)^{-\frac{1}{2}} \rho_i \left(\sum_{j=1}^{N} \rho_j\right)^{-\frac{1}{2}}.$$

This measurement is useful for two reasons. First it is directly defined in terms of the states to distinguish. Secondly, the pretty good measurement is involved in many bounds which can themselves be used to bound the optimal probability of success. These bounds are often easier to evaluate than the success probability itself. For instance, Barnum and Knill [8] showed that

$$p_{succ}^{PGM} \geq (p_{succ}^{optimal})^2$$

where p_{succ}^{PGM} is the probability of success of the PGM. This measurement will appear frequently in this thesis.

---

[3]It performs "fairly well" in the sense that the mutual information between the probability distribution of the states and the probability distribution of the outcomes from the measurement has a vanishing gradient in terms of the variations of the measurement basis.

3 Quantum information with continuous variables

Quantum information processing can be done in two ways, digitally (nuclear spins, photon polarization...) or analogously (position, momentum...). In the latter case, the information is encoded in a system with infinitely many degrees of freedom. A typical example is quantum optics, where photons are used as information carriers. This section will focus on the different mathematical tools to represent some of the resources used in quantum optics which are described by continuous variables. Again, we refer the reader to [28, 29] for more information.

3.1 Quantization of the electrical field

In quantum optics, every quantum state is related to an electrical field and so we start by introducing quantized fields and the quantum states arising from them. Assuming the classical electrical field is restricted to some volume with appropriate boundary conditions, Maxwell's equations offer a solution for the expression of this field

$$\vec{E}(\vec{r}, t) = \sum_k \left(c_k \vec{u}_k(\vec{r}) e^{-i\omega_k t} + c_k^* \vec{u}_k^*(\vec{r}) e^{i\omega_k t} \right)$$

where $\{\vec{u}_k\}$ are a discrete set of orthogonal mode functions respecting the boundary conditions of the problem and the constants $\{c_k\}$ are the Fourier coefficients of the decomposition of the electrical field. The idea behind the quantization of the electrical field is to have the field promoted to operators. This is done by replacing the Fourier coefficients $\{c_k\}$ characterizing the presence of each mode in the overall field by creation and annihilation $\{a_k^\dagger, a_k\}$ operators describing the quantum modes in the overall field

$$\vec{E}(\vec{r}, t) \propto \sum_k \left(a_k \vec{u}_k(\vec{r}) e^{-i\omega_k t} + a_k^\dagger \vec{u}_k^*(\vec{r}) e^{i\omega_k t} \right) \tag{9}$$

14

where a proportionality constant has been introduced to make a_k and $a_k^\dagger$ dimensionless. Photons being bosons, the commutation relation for the a_k and $a_k^\dagger$ should be

$$[a_k, a_k^\dagger] = \mathbb{1} \qquad \text{and} \qquad [a_j, a_k^\dagger] = 0 \ (j \neq k) \tag{10}$$

so operators associated with different modes commute. The energy of the electromagnetic field ($\vec{H}$ being the magnetic field) is given by

$$E = \frac{1}{2} \int \left(\epsilon_0 \|\vec{E}\|^2 + \mu_0 \|\vec{H}\|^2 \right) d\vec{r}$$

and this implies using (9) that the Hamiltonian is

$$H = \sum_k \hbar \omega_k \left(a_k^\dagger a_k + \frac{1}{2} \right).$$

In other words, every mode constitutes a quantum harmonic oscillator. Quantum optics usually refers to the different quadratures of a mode

$$x_k = \frac{1}{\sqrt{2}} (a_k + a_k^\dagger) \qquad \text{and} \qquad p_k = \frac{-i}{\sqrt{2}} (a_k - a_k^\dagger) \tag{11}$$

whose interpretation can be seen by reexpressing (9) in the case of a plane wave for a single mode

$$\vec{E}(\vec{r}, t) \propto x_k \cos(\omega_k t - \vec{k} \cdot \vec{r}) + p_k \sin(\omega_k t - \vec{k} \cdot \vec{r}).$$

From this expression we see that x_k and p_k are the "in phase" component and "out of phase" component of the electrical field.

3.2 One mode states

3.2.1 Coherent states and displacement operators

The harmonic oscillator is usually treated using the Fock basis, also known as the number basis $\{|n\rangle\}_{n\in\mathbb{N}_0}$ i.e. eigenstates of the number operator $a^\dagger a$. We have the eigenvalue equation

$$a^\dagger a|n\rangle = n|n\rangle \qquad \text{for} \qquad n \in \mathbb{N}_0. \tag{12}$$

The state $|0\rangle$ is the vacuum state and is determined up to a phase by $a|0\rangle = 0$. Fock basis states are useful in the mathematical treatment of the harmonic oscillator but they are difficult to generate with quantum optics tools (with the exception of the vacuum). A more suitable candidate to work with is the coherent state, which describes the light emitted from a laser. Coherent states, denoted $|\alpha\rangle$, are defined $\forall \alpha \in \mathbb{C}$ as eigenstates of the annihilation operator

$$a|\alpha\rangle = \alpha|\alpha\rangle$$

where α can be complex because a is not Hermitian. Alternatively, coherent states can be defined by the displacement operator

$$D(\alpha) = \exp(\alpha a^\dagger - \alpha^* a) \tag{13}$$

as displacement from the vacuum state

$$|\alpha\rangle = D(\alpha)|0\rangle.$$

16

The operators $D(\alpha)$ are unitary

$$D^{-1}(\alpha) = D^\dagger(\alpha) = D(-\alpha),$$

and their action on the creation and annihilation operators is

$$D^\dagger(\alpha)aD(\alpha) = a + \alpha\mathbb{1} \qquad \text{and} \qquad D^\dagger(\alpha)a^\dagger D(\alpha) = a^\dagger + \alpha^*\mathbb{1}. \tag{14}$$

This allows us to see how the quadratures (11) are affected by a displacement $D(\alpha)$:

$$D^\dagger(\alpha)xD(\alpha) = x + \sqrt{2}Re(\alpha)\mathbb{1} \qquad \text{and} \qquad D^\dagger(\alpha)pD(\alpha) = p + \sqrt{2}Im(\alpha)\mathbb{1}.$$

Therefore the displacement operators translate any state in the phase space (x, p). These relations can also be used to show that coherent states are eigenstates of the operator a because

$$a|\alpha\rangle = D(\alpha)D^\dagger(\alpha)aD(\alpha)|0\rangle = D(\alpha)(a + \alpha)|0\rangle = \alpha|\alpha\rangle$$

where we used the unitarity of $D(\alpha)$, equations (13) and (14). It is possible to express coherent states as a superposition in the number basis

$$|\alpha\rangle = e^{-\frac{|\alpha|^2}{2}} \sum_n \frac{\alpha^n}{\sqrt{n!}}|n\rangle \tag{15}$$

which can be used to infer some other properties of coherent states. For instance, we can see that a coherent state has a mean photon number $\langle\alpha|a^\dagger a|\alpha\rangle = |\alpha|^2$. Also, coherent states form a basis of the Hilbert space in the sense that

$$\frac{1}{\pi} \int |\alpha\rangle\langle\alpha|d^2\alpha = \mathbb{1}$$

17
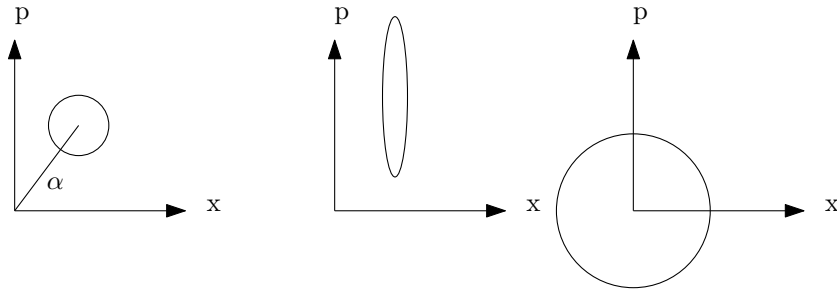
Figure 1: Illustrated on the plane (x, p) of the phase space, coherent states (left graph) are represented by a point of coordinates $\sqrt{2}(Re(\alpha), Im(\alpha))$ centered in a circle of radius $\frac{1}{2}$ for the variance. The uncertainty of squeezed states (middle graph) is given by an ellipse squeezed along the appropriate quadrature (p in this case). Thermal states (right graph) are centered around the origin with circle variance with radius greater than $\frac{1}{2}$.

($d^2\alpha$ being the Lebesgue measure on $\mathbb{C}^2$) but it is an overcomplete basis since different coherent states are non-orthogonal,

$$|\langle \beta | \alpha \rangle|^2 = e^{-|\alpha - \beta|^2} \qquad \text{for} \qquad \alpha, \beta \in \mathbb{C}.$$

Coherent states are also sometimes called quasi-classical states for the following reason. Heisenberg's uncertainty principle tells us the standard deviations of the quadratures $\Delta x := \sqrt{\langle (x - \langle x \rangle)^2 \rangle}$ and $\Delta p := \sqrt{\langle (p - \langle p \rangle)^2 \rangle}$ in any state $|\psi\rangle$ satisfy the fundamental relation

$$\Delta x \Delta p \geq \frac{1}{2}. \tag{16}$$

(Here $\langle A \rangle$ denotes the expectation value $\langle \psi | A | \psi \rangle$.) Computing $\Delta x \Delta p$ with the definition of the quadratures (11) shows that the bound is saturated for coherent states. Therefore, they are states of minimum uncertainty and in this sense can be seen as best characterized in the phase space. In Figure 1, we illustrate some examples of one mode states in the phase space.

3.2.2 Squeezed states

Note that the uncertainty in either of the quadratures is not constrained, only their product is by equation (16). It is natural to expect that one may reduce the uncertainty in one quadrature at the cost of an increase in the uncertainty of the other quadrature. Squeezed states are an example of states with this feature. They can be generated from the vacuum by applying the squeezing operator

$$S(\zeta) = \exp\left(\frac{\zeta^* a^2 - \zeta a^{\dagger 2}}{2}\right)$$

where $\zeta = re^{i\phi}$. In general, a squeezed state can also be displaced, in which case it is denoted by $|\alpha, \zeta\rangle := D(\alpha)S(\zeta)|0\rangle$. Squeezing transforms the creation and annihilation operators as follows

$$S^\dagger(\zeta)aS(\zeta) = a\cosh r - a^\dagger e^{i\phi}\sinh r \qquad \text{and} \qquad S^\dagger(\zeta)a^\dagger S(\zeta) = a^\dagger \cosh r - ae^{-i\phi}\sinh r.$$

In the case where ζ is real, the quadratures are mapped to

$$S^\dagger(\zeta)xS(\zeta) = e^{-r}x \qquad \text{and} \qquad S^\dagger(\zeta)pS(\zeta) = e^r p. \tag{17}$$

Using (17), we can conclude that the uncertainties are affected by this transformation as follows

$$\Delta x \to e^{-r}\Delta x \qquad \text{and} \qquad \Delta p \to e^r \Delta p.$$

It is clear now that the product of the uncertainties remains invariant under a squeezing transformation although the uncertainty in each quadrature changes. In the limit where $r \to \infty$, the squeezed state $|\alpha, r\rangle$ is then perfectly defined on its x quadrature while the p quadrature becomes

19

completely random. This is a (at least conceptual) tool to generate eigenstates of the quadratures

$$|x\rangle = \lim_{r\to\infty} D\left(\frac{x}{\sqrt{2}}\right) S(r)|0\rangle \qquad \text{and} \qquad |p\rangle = \lim_{r\to\infty} D\left(i\frac{p}{\sqrt{2}}\right) S(-r)|0\rangle.$$

However this statement is a little bit misleading, because the calculation of the expectation value for the number of photons $\langle n \rangle = \langle a^\dagger a \rangle$ yields

$$\langle n \rangle = \langle \alpha, \zeta | a^\dagger a | \alpha, \zeta \rangle = |\alpha|^2 + \sinh^2 r$$

which diverges if $r \to \infty$. In fact $|x\rangle$ and $|p\rangle$ are non-normalizable and hence non-physical states. They will be mostly used as a convenient conceptual tool when trying to measure the x or p quadrature by projecting on relevant eigenstates, but it should be kept in mind that this is an idealization. As a matter of fact, the error that might be present in real life applications can be modeled by assuming imperfect squeezing of the resources used.

3.2.3 Thermal states

Coherent states and squeezed states saturate Heisenberg's uncertainty relation (16) i.e. their combined uncertainties in their quadratures are minimal. An important example of a state that does not have minimal uncertainty is a thermal state. It can be represented as a Gaussian mixture of coherent states

$$\rho_N = \frac{1}{\pi N} \int e^{\frac{-|\alpha|^2}{N}} |\alpha\rangle\langle\alpha| d^2\alpha. \tag{18}$$

The value of N represents the mean photon number in the thermal state. It has zero displacement as one may intuitively expect from the fact that the Gaussian distribution is rotationally invariant in phase space (it only depends on the norm of α). It has non-minimal uncertainty since the

distribution spreads over all the phase space (with variance $N/2$) even though the thermal state has zero displacement. Both of the quadratures have a variance

$$\Delta x = \Delta p = N + \frac{1}{2}$$

which can be arbitrarily large depending on the mean photon number. The matrix elements of ρ_N in the Fock basis are given by

$$\langle n|\rho_N|m\rangle = \delta_{nm}\frac{1}{N+1}\left(\frac{N}{N+1}\right)^n.$$

This means that ρ_N is diagonal in the same basis as the number operator $a^\dagger a$ and therefore they commute. Defining $N = (e^\beta - 1)^{-1}$, we can rewrite the thermal state as

$$\rho_{thermal} = \frac{e^{-\beta a^\dagger a}}{\mathsf{tr}(e^{-\beta a^\dagger a})}$$

and the relation to canonical ensembles in statistical mechanics becomes obvious. This state can be thought of as a state in thermal equilibrium at temperature $1/\beta$ determining the spread in the Gaussian distribution in (18).

3.3 Gaussian states

In the last section, important quantum states in quantum optics have been studied without a general framework. This was sufficient because the states had nice properties, but this will not always be the case. For this reason, it is necessary to develop tools to analyse more general states. One way to begin this presentation is to exploit the idea that density operators represent some sort of generalized probability distribution representing physical systems. To motivate the definition of Gaussian characteristic functions and states [28] , let us first discuss analogous concepts for classical

probability distributions.

3.3.1 Characteristic functions

Given a probability distribution $p(x)$ over $\mathbb{R}$, its characteristic function $\phi_X(t)$ is given as the expectation value of e^{itX} (or equivalently as the Fourier transform of the probability distribution)

$$\phi_X(t) = E[e^{itX}] = \int p(x)e^{itx}dx. \tag{19}$$

The characteristic function is useful because it generates all the moments from the probability distribution via the following formula

$$E[X^k] = i^k \frac{\partial^k}{\partial t^k}\phi_X(t)\bigg|_{t=0}.$$

A probability distribution is completely defined by its moments and therefore by its characteristic function. In fact, one can recover the probability distribution $p(x)$ directly from $\phi_X(t)$ by inverting the Fourier transform

$$p(x) = \frac{1}{2\pi} \int \phi_X(t)e^{-itx}dt. \tag{20}$$

The extension of this concept to quantum states requires us to define the Weyl operators. Consider a system of n modes with mode operators $\{a_j, a_j^\dagger\}_{j=1}^n$ satisfying the canonical commutation relations (10). Define the Weyl operators

$$W_\xi = e^{-i\xi^T \sigma r} \qquad \text{for} \qquad \xi \in \mathbb{R}^{2n}.$$

Here σ is the block diagonal matrix $\sigma = \bigoplus_{i=1}^n \begin{pmatrix} 0 & 1 \\ -1 & 0 \end{pmatrix}$ and $r = (x_1, p_1, ..., x_n, p_n)$ is a vector of

operators representing the quadratures in the different modes (cf. (11)).[4] Weyl operators can be multiplied using the following relation

$$W_\xi W_\eta = e^{-\frac{1}{2}\xi^T \sigma \eta} W_{\xi+\eta}.$$

and they respect the orthogonality relation

$$\text{tr}[W_{-\xi} W_\eta] = (2\pi)^n \delta^{(2n)}(\xi - \eta)$$

where $\delta^{(2n)}(\xi)$ is the Dirac delta in $\mathbb{R}^{2n}$.

The characteristic function χ_ρ of a quantum state ρ is defined as the expectation value of the Weyl operator W_ξ:

$$\chi_\rho(\xi) = \text{tr}(\rho W_\xi), \quad \xi \in \mathbb{R}^{2n}.$$

This expression is the quantum analog of (19). It is possible to recover the state from its characteristic function (in the same sense it is possible to invert the Fourier transform, (20))

$$\rho = \frac{1}{(2\pi)^n} \int d^{2n}\xi \chi_\rho(-\xi) W_\xi. \tag{21}$$

This relation will be useful in the following sections.

3.3.2 Gaussian characteristic functions

For a classical Gaussian distribution $p(x) = e^{-\frac{(x-\mu)^2}{2\sigma^2}}$, the characteristic function is given by

$$\phi_X(t) = \exp\left(-\frac{1}{2}\sigma^2 t^2 + i\mu t\right)$$

---

[4]This notation offers a compact way to express the commutation relations between the quadratures: $[r_k, r_l] = i\sigma_{kl}$.

with first moment μ and second moment $\mu^2 + \sigma^2$. Since this characteristic function is uniquely defined by its first and second moments, the variance and the mean are all that is needed to completely describe a Gaussian distribution. It is with this idea in mind that we define a Gaussian characteristic function for quantum states. A quantum state is said to be a Gaussian state if its characteristic function has the form

$$\chi_\rho(\xi) = \exp(-\frac{1}{4}\xi^T \sigma^T \gamma \sigma \xi - id^T \sigma \xi). \tag{22}$$

In this formula, $d \in \mathbb{R}^{2n}$ is called the displacement vector of the Gaussian state and is given by

$$d_i = \mathsf{tr}(\rho r_i).$$

If $d_i = 0 \quad \forall i$, we will say that ρ is a centered Gaussian state. The matrix γ is a $2n \times 2n$ matrix called the covariance matrix. It is given by

$$\gamma_{ij} = \mathsf{tr}\left[\rho \left\{r_i - d_i, r_j - d_j\right\}\right]$$

where $\{A, B\} = AB + BA$.

Consider a Weyl operator W_ξ acting on one mode only, then the argument of the exponential can be expanded as

$$W_\xi = e^{-i(\xi_1 p - \xi_2 x)} = e^{\frac{1}{\sqrt{2}}\left((\xi_1 + i\xi_2)a^\dagger - (\xi_1 - i\xi_2)a\right)}.$$

Then it is obvious that the Weyl operator is just another form of the displacement operator (13), $W_\xi = D(\frac{1}{\sqrt{2}}(\xi_1 + i\xi_2))$. This makes the calculation of the characteristic function for coherent states and squeezed states much easier. In fact, coherent states, displaced squeezed states and thermal states are three important examples of Gaussian states. For a coherent state $|\alpha\rangle$ (cf. (13)), the

covariance matrix and the displacement vector are

$$\gamma_\alpha = \mathbb{1} \qquad \text{and} \qquad d_\alpha = \sqrt{2}(Re(\alpha), Im(\alpha))^T. \qquad (23)$$

For a one mode squeezed state $|\psi\rangle = |\alpha, r\rangle$, it reads

$$\gamma_\psi = \begin{pmatrix} e^{-2r} & 0 \\ 0 & e_{2r} \end{pmatrix} \qquad \text{and} \qquad d_\psi = \sqrt{2}(Re(\alpha), Im(\alpha))^T.$$

For a thermal state ρ_N we have

$$\gamma_N = (2N+1)\mathbb{1} \qquad \text{and} \qquad d_N = (0,0)^T.$$

3.4   Gaussian operations

We have discussed the formalism for representing states arising in many protocols of interest. It remains to describe how this representation transforms when we operate on the states. This is the focus of the present section. The most relevant operations for this work are Gaussian operations i.e. operations $\mathcal{E}$ that sends Gaussian states to Gaussian states.

3.4.1   Gaussian unitaries

Consider first the special case where the operation $\mathcal{E}(\rho) = U\rho U^\dagger$ is evolution under a unitary U. If the unitary preserves the property of being Gaussian, we call U a Gaussian unitary. These unitaries arise from Hamiltonians which are quadratic in the mode operators. It can be intuitively understood because higher order terms would affect higher than second-order moments. Gaussian unitaries are convenient because of the following theorem which is a consequence of the Stone-von Neumann theorem [29].

Theorem 3.1 (Metaplectic representation) *Given a symplectic transformation S (a symplectic transformation preserves σ, $S\sigma S^T = \sigma$) and $\mathcal{H}$ the Hilbert space the Weyl operators act on, there exists a unique Gaussian unitary U_S (up to a phase) acting on $\mathcal{H}$ such that*

$$U_S W_\xi U_S^\dagger = W_{S\xi}. \tag{24}$$

Conversely, every Gaussian unitary U acts on Weyl operators as (24) for some symplectic transformation S. More explicitly, it is always possible to interpret a Gaussian transformation on a quantum states as a transformation acting on the quadratures. By looking at the expression for the characteristic function, it should be clear that such a transformation can also be written on the covariance matrix and displacement vector

$$\gamma \to S^T \gamma S \qquad \text{and} \qquad d \to S^T d.$$

It is this last description of the effect of a Gaussian unitary that we will use most often.

It is possible to describe a general n mode symplectic transformation in an intuitive manner by the results shown in [13, 14] . It says that any symplectic transformation S can be decomposed by a multi-mode beam-splitter represented by the matrix K followed by simultaneous single-mode squeezers with parameters $\{s_i\}$ and another multi-mode beam-splitter represented by the matrix L

$$S = K \bigoplus_{i=1}^{n} \begin{pmatrix} e^{-s_i} & 0 \\ 0 & e^{s_i} \end{pmatrix} L.$$

This formulation is especially useful when combined with Williamson theorem [15].

Theorem 3.2 (Williamson theorem) *Every real and positive definite $2n \times 2n$ matrix γ can be*

diagonalized by a symplectic transformation S such that

$$S\gamma S^T = \bigoplus_{i=1}^{n} \begin{pmatrix} \nu_k & 0 \\ 0 & \nu_k \end{pmatrix}.$$

This diagonalized form should be recognized as the covariance matrix of a n mode thermal state. Since this applies to every covariance matrix possible, that means it is possible to generate any Gaussian state by having a n mode thermal state and applying in succession a beam-splitter, one mode squeezing on each mode and another beam-splitter before applying the appropriate displacement. This is called the normal mode decomposition.

3.4.2   Gaussian channels

A more general Gaussian operation i.e. a CPTP map $\mathcal{E}$ preserving Gaussianity is also characterized by its action on the covariance matrix and displacement vector of the input state. This action can be expressed as

$$\gamma \rightarrow X\gamma X^T + Y \qquad \text{and} \qquad d \rightarrow Xd.$$

Here X and Y are real $2n \times 2n$ matrices. The X part of the transformation represents more or less everything that might be considered amplification, attenuation or rotation in the phase space while Y represents noise introduced by the use of the channel. This noise is often necessary to make the channel physical because complete positivity of $\mathcal{E}$ implies a relation which must be respected by X and Y [30]

$$Y + i\sigma - iX\sigma X^T \geq 0.$$

3.4.3 Examples

Partial trace The reduced density operator ρ_A after tracing out part of a multi-partite Gaussian state ρ_{AB} is still a Gaussian state. This implies that the partial trace $\mathcal{E}(\rho_{AB}) = \mathsf{tr}_B(\rho_{AB})$ is a Gaussian operation. The action on the covariance matrix and displacement is quite simple: assume the covariance matrix has the block form

$$\gamma_{AB} = \begin{pmatrix} \gamma_A & \delta_{AB} \\ \delta_{AB}^T & \gamma_B \end{pmatrix}$$

and the displacement is the combination

$$d_{AB} = (d_A, d_B)^T.$$

The characteristic function of the reduced density operator ρ_A is then simply γ_A and d_A.

The same idea can be used to find the covariance matrix of the joint product state of two Gaussian states. If ρ_A has covariance matrix γ_A and displacement d_A and ρ_B has covariance matrix γ_B and displacement d_B, then the state $\rho_A \otimes \rho_B$ has block diagonal covariance matrix $\gamma_A \oplus \gamma_B$ and displacement $(d_A, d_B)^T$.

Beam-splitter All the operations that are covered in this section are related to actual operations that can be performed in a quantum optics lab. One example of a device inducing such an operation is a beam-splitter with transmittivity T. Its action is well understood; a beam of light goes through a semi-transparent mirror such that part of the photons are reflected by the mirror and the leftover part goes through the mirror unaffected. It is possible to combine two beams of light using this technique, the reflected part of the first beam is combined with the unaffected part of the second beam and vice versa. This operation is described by a Gaussian unitary U with an associated

symplectic transformation S acting on the quadratures as follow

$$\begin{pmatrix} r_1 \\ r_2 \end{pmatrix}_{out} = \begin{pmatrix} \sqrt{T}\mathbb{1} & \sqrt{1-T}\mathbb{1} \\ -\sqrt{1-T}\mathbb{1} & \sqrt{T}\mathbb{1} \end{pmatrix} \begin{pmatrix} r_1 \\ r_2 \end{pmatrix}_{in}. \tag{25}$$

r_1 and r_2 are the quadrature vectors $(x, p)^T$ for mode 1 and mode 2 respectively and $\mathbb{1}$ is the 2×2 identity matrix. A different, but physically equivalent, convention is to have the minus sign on the upper right entry instead of the lower left entry. The most common occurrence of a beam-splitter is given for $T = \frac{1}{2}$, this is when the same amount of light is transmitted and reflected by the semi-transparent mirror. For this reason it is referred to as a 50:50 beam-splitter.

Quadrature measurement Quadrature measurement is a measurement which is commonly considered in quantum optics. The goal is to measure the observable $Re(\alpha)x + Im(\alpha)p$ for some $\alpha \in \mathbb{C}$. Usually we will take the special case where α is purely real or purely imaginary. We will explain how to do this with beam-splitters and photon detectors.

Suppose the mode to be detected is described by creation and annihilation operators a and $a^\dagger$. The first step is to combine the mode to be measured with a strong local oscillator using a 50:50 beam-splitter. A strong local oscillator is a beam of light in a coherent state $|\alpha\rangle$ with a high mean photon number $|\alpha|^2$. Because of this, the local oscillator can be treated classically using a complex amplitude α rather than creation/annihilation operators. After the beam-splitter, the operators of the modified modes are given by (in the Heisenberg picture)

$$a_1 = \frac{\alpha\mathbb{1} + a}{\sqrt{2}} \qquad \text{and} \qquad a_2 = \frac{\alpha\mathbb{1} - a}{\sqrt{2}}.$$

The intensities of the modes are then measured by two photodiodes which convert light intensity into an electrical current. Measuring this current i_1, i_2 for the two modes is then equivalent to

measuring

$$i_1 \propto n = a_1^\dagger a_1 = (\alpha^* + a^\dagger)(\alpha + a)/2 \qquad \text{and} \qquad i_2 \propto n = a_2^\dagger a_2 = (\alpha^* - a^\dagger)(\alpha - a)/2.$$

Looking at the difference between these two currents, one can see that

$$\delta i = i_1 - i_2 \propto (\alpha^* a + \alpha a^\dagger).$$

Taking an appropriate value for the phase of $\alpha = |\alpha| e^{i\theta}$, it is possible to measure any linear combination of the creation and annihilation operator. In particular, taking the phase $\theta = 0$ will produce a measurement of the x quadrature and the phase $\theta = \frac{\pi}{2}$ will give a measurement of the quadrature p. The measurement of the x or p quadrature is called a homodyne measurement.

3.4.4 Projective measurement

More generally, a measurement can involve a projection on some arbitrary pure state $|\psi\rangle$ and could be applied to some arbitrary modes of a multimode state ρ. The corresponding probability and post-measurement state are determined by the following lemma.

Lemma 3.3 (Projective measurement on Gaussian states) *Let ρ_{AB} be a state of $n_A + n_B$ modes on systems A and B, and let $|\psi\rangle_B$ be a pure state on B. Consider a POVM which has an element proportional to $|\psi\rangle\langle\psi|_B$. Denote by $\tilde{\rho}_A = \mathsf{tr}_B((\mathbb{1}_A \otimes |\psi\rangle\langle\psi|_B)\rho_{AB})/p(\psi)$ the normalized post-measurement state on A after performing a measurement on B with outcome $|\psi\rangle$ and $p(\psi) = \mathsf{tr}_{AB}((\mathbb{1}_A \otimes |\psi\rangle\langle\psi|_B)\rho_{AB})$ the normalization. Then*

$$\chi_{\tilde{\rho}_A}(\xi) = \frac{1}{(2\pi)^{n_B} p(\psi)} \int \chi_{\rho_{AB}}(\xi, \eta) \chi_{|\psi\rangle\langle\psi|}(-\eta) d^2\eta \qquad \textit{for all } \xi \in \mathbb{R}^{2n_A}. \tag{26}$$

In particular, if ρ_{AB} is Gaussian with covariance matrix and displacement

$$\gamma_{AB} = \begin{pmatrix} \gamma_A & \delta_{AB} \\ \delta_{AB}^T & \gamma_B \end{pmatrix} \qquad d_{AB} = (d_A, d_B) \in \mathbb{R}^{2n_A} \times \mathbb{R}^{2n_B} \ , \tag{27}$$

and $|\psi\rangle$ is Gaussian with covariance matrix γ_ψ and displacement d_ψ, then $\tilde{\rho}_A$ is Gaussian with covariance matrix

$$\tilde{\gamma} = \gamma_A - \delta_{AB}(\gamma_B + \gamma_\psi)^{-1}\delta_{AB}^T$$

and displacement

$$\tilde{d}_A = d_A + \delta_{AB}(\gamma_B + \gamma_\psi)^{-1}(d_\psi - d_B).$$

Furthermore the probability of obtaining the outcome associated with the POVM element $|\psi\rangle\langle\psi|$ is

$$p(\psi) = \frac{1}{\pi^{n_B}\sqrt{\det(\gamma_B + \gamma_\psi)}} \exp\left(-(d_\psi - d_B)^T(\gamma_B + \gamma_\psi)^{-1}(d_\psi - d_B)\right)$$

where d_ψ is the displacement vector of $|\psi\rangle\langle\psi|$.

We present the proof in Appendix A.

The result of a measurement on a Gaussian state can be used to make conditional operations on the post-measurement state. Consider for example the POVM $\{E_m d^{2n_B} m\}$ with the rank-one operators

$$E_m = \frac{1}{(2\pi)^{2n_B}} D(m)|\psi\rangle\langle\psi|D(m)^\dagger \qquad m \in \mathbb{C} \tag{28}$$

where $|\psi\rangle$ is an arbitrary pure state of n_B modes and $d^{2n_B}m$ is the Lebesque measure on $\mathbb{R}^{2n_B}$. Then the following statement extends Lemma 3.3.

Lemma 3.4 (Average state for conditional displacement) *Suppose $|\psi\rangle$ is the centered Gaussian state of (28) with covariance matrix γ_ψ. Fix some linear map $\Gamma : \mathbb{R}^{2n_B} \to \mathbb{R}^{2n_A}$ and consider the following process:*

1. *Measure the system B of ρ_{AB} using the POVM on B defined by (28), getting outcome $m \in \mathbb{R}^{2n_B}$.*

2. *Apply $D(\Gamma m)$ to A.*

In other words, this process is described by the CPTP map $\mathcal{E} : \mathcal{B}(A \otimes B) \to \mathcal{B}(A)$ defined by

$$\mathcal{E}(\rho_{AB}) = \int D(\Gamma m)\mathsf{tr}_B((\mathbb{1}_A \otimes E_B^m)\rho_{AB})D(\Gamma m)^\dagger d^{2n_B}m. \tag{29}$$

Let ρ_{AB} be a Gaussian state of $n_A + n_B$ modes with covariance matrix and displacement as in (27). Then the state $\mathcal{E}(\rho_{AB})$ resulting from this process is Gaussian with covariance matrix and displacement

$$\tilde{\gamma}_A = \gamma_A + \Gamma(\gamma_B + \gamma_\psi)\Gamma^T + \Gamma\delta_{AB}^T + \delta_{AB}\Gamma^T$$
$$\tilde{d}_A = d_A + \Gamma d_B.$$

We present the proof of this lemma in Appendix B.

3.4.5 Homodyne measurement

As a special case of Lemma 3.3, it is possible to get an expression for the covariance matrix of the post-measurement state after homodyne measurement. The main challenge of this calculation is

that the projection on quadrature states is an idealization and this requires to consider the limit of infinite squeezing.

Corollary 3.5 (Homodyne measurement) *Assume we have a Gaussian state ρ_{AB} (here A consists of n modes and B is one mode) with covariance matrix γ_{AB} and displacement d_{AB} as defined in Lemma 3.3. After doing a measurement of the x quadrature on the last mode B, the covariance matrix and displacement of the post-measurement state is given by*

$$\tilde{\gamma} = \gamma_A - \delta_{AB}(\pi_x \gamma_B \pi_x)^{-1} \delta_{AB}^T$$

where $\pi_x = \begin{pmatrix} 1 & 0 \\ 0 & 0 \end{pmatrix}$. The displacement is given by

$$\tilde{d} = d_A + \frac{x - d_{B1}}{\gamma_{B11}} [\delta_{AB}]_1 \tag{30}$$

where $[\delta_{AB}]_1$ is the column vector obtained by taking the first column of δ_{AB} while γ_{B11} and d_{B1} represent specific entries of the matrix and vector respectively. A measurement of the p quadrature produces the same result, with π_x replaced by $\pi_p = \begin{pmatrix} 0 & 0 \\ 0 & 1 \end{pmatrix}$ and all indices 1 by 2 in (30).

Proof Assuming $\gamma_B = \begin{pmatrix} B_{11} & B_{12} \\ B_{21} & B_{22} \end{pmatrix}$, the calculation of the new covariance matrix involves the

following factor (see lemma 3.3)

$$(\gamma_B + \gamma_\psi)^{-1} = \lim_{r \to \infty} \left[\begin{pmatrix} B_{11} & B_{12} \\ B_{21} & B_{22} \end{pmatrix} + \begin{pmatrix} e^{-2r'} & 0 \\ 0 & e^{2r'} \end{pmatrix} \right]^{-1}$$

$$= \lim_{r \to \infty} \frac{1}{(B_{11} + e^{-2r'})(B_{22} + e^{2r'}) - B_{12}B_{21}} \begin{pmatrix} B_{22} + e^{2r'} & -B_{21} \\ -B_{12} & B_{11}e^{-2r'} \end{pmatrix}$$

$$= \begin{pmatrix} \frac{1}{B_{11}} & 0 \\ 0 & 0 \end{pmatrix} \tag{31}$$

which leads to the simplified form for the covariance matrix

$$\tilde{\gamma} = \gamma_A - \delta_{AB}(\pi_x \gamma_B \pi_x)^{-1} \delta_{AB}^T$$

where $\pi_x = \begin{pmatrix} 1 & 0 \\ 0 & 0 \end{pmatrix}$ and the inverse is defined on the support of the matrix. There also is a nice simplification for the displacement of the post-measurement state. Because of the form of (31), it is fairly easy to compute $\delta_{AB}(\gamma_B + \gamma_\psi)^{-1}$. This produces the final result

$$\tilde{d} = d_A + \frac{x - d_{B1}}{\gamma_{B11}} [\delta_{AB}]_1$$

with $[\delta_{AB}]_1$ being a column vector when only considering the first column of δ_{AB}.

The case of the measurement of $|p\rangle\langle p|$ is very similar. The squeezing is now in the perpendicular direction from the x quadrature case. The calculation used for the measurement of x can simply be modified by taking the limit $r \to -\infty$ instead of $r \to +\infty$. In this case, the result is that the covariance matrix of the post-measurement state is

$$\tilde{\gamma} = \gamma_A - \delta_{AB}(\pi_p \gamma_B \pi_p)^{-1} \delta_{AB}^T$$

where $\pi_p = \begin{pmatrix} 0 & 0 \\ 0 & 1 \end{pmatrix}$. Then it is trivial to see that the indices 1 will be replaced by 2 and x by p in (30). ∎

3.5 Entanglement for two-mode states

The most popular example of entanglement between two qubit systems is given by the Bell states

$$|\Phi_2^+\rangle = \frac{1}{\sqrt{2}}(|00\rangle + |11\rangle)$$

$$|\Phi_2^-\rangle = \frac{1}{\sqrt{2}}(|00\rangle - |11\rangle)$$

$$|\Psi_2^+\rangle = \frac{1}{\sqrt{2}}(|01\rangle + |10\rangle)$$

$$|\Psi_2^-\rangle = \frac{1}{\sqrt{2}}(|01\rangle - |10\rangle).$$

Entanglement is also available in quantum optics and is in fact crucial for the protocols that will be studied in the subsequent sections, but it usually comes in a different form. The immediate naive generalization of $|\Phi_2^+\rangle$ to infinite-dimensional (as the superposition of correlated kets on two subsystems) is

$$\int |x\rangle|x\rangle dx = \int \delta(x - y)|x\rangle|y\rangle dx dy$$

so the wave function is $\psi(x_1, x_2) = C\delta(x_1 - x_2)$. This represents a two-mode state perfectly correlated in position ($x_1 = x_2$) and anticorrelated in momentum ($p_1 + p_2 = 0$). This, however, is not a physical state since it is not normalizable. Therefore we only have "approximate" maximal entanglement when we consider infinite-dimensional states.

In a finite-dimensional setting, the CNOT gate is used as an entangling gate. Indeed, using this gate on the separable state $\frac{|00\rangle + |10\rangle}{\sqrt{2}}$ will yield the inseparable and hence entangled state $|\Phi_2^+\rangle$.

The CNOT gate makes sense when working with qubits, but we do not have an unambiguous generalization for continuous variables. We must use other resources to generate entanglement for infinite-dimensional systems. We will now show how to do this with operators common in quantum optics. Using the Heisenberg picture, we start with two two-mode system with quadratures x_1, p_1 and x_2, p_2 and we want to show that at the end of the procedure, the quadratures are correlated in x $(x_1 = x_2)$ and anti-correlated in p $(p_1 = -p_2)$.

The state with these properties will be called a two-mode squeezed state. We will create this state by introducing separate squeezing on the individual modes and then applying a 50:50 beam-splitter. Intuitively, the squeezing should allow us to control the quality of entanglement by enhancing the correlations of the quadratures. The beam-splitter, by forcing the description of each new mode as a combination from the initial ones, should act as our entangling operator. Squeezing the first mode in p and the second mode in x gives

$$a_1' = \cosh r\, a_1 + \sinh r\, a_1^\dagger \qquad \text{and} \qquad a_2' = \cosh r\, a_2 - \sinh r\, a_2^\dagger$$

and then applying the beam-splitter

$$a_1'' = (a_1' + a_2')/\sqrt{2} \qquad \text{and} \qquad a_2'' = (a_1' - a_2')/\sqrt{2}$$

and upon combining these operators to obtain the quadratures at the output yields

$$x_1'' = (e^r x_1 + e^{-r} x_2)/\sqrt{2} \qquad \text{and} \qquad x_2'' = (e^r x_1 - e^{-r} x_2)/\sqrt{2}$$
$$p_1'' = (e^{-r} p_1 + e^r p_2)/\sqrt{2} \qquad \text{and} \qquad p_2'' = (e^{-r} p_1 - e^r p_2)/\sqrt{2}.$$

From these quadratures, it is evident that each one of them individually only get noisier (the variance acquires an exponential factor) when the squeezing is large, but the relative position and

total momentum however

$$x_1'' - x_2'' = \sqrt{2}e^{-r}x_2 \qquad \text{and} \qquad p_1'' + p_2'' = \sqrt{2}e^{-r}p_1$$

become well-defined, $\langle (x_1'' - x_2'')^2 \rangle = e^{-2r}/2$, $\langle (p_1'' + p_2'')^2 \rangle = e^{-2r}/2$ as we wanted.

Formally, the entanglement generating process can be represented by a single operator, the two-mode squeezing operator (with $\zeta = re^{i\theta}$), applied on a two-mode vacuum state $|0\rangle \otimes |0\rangle$

$$S_2(\zeta) = \exp(\zeta^* a_1 a_2 + \zeta a_1^\dagger a_2^\dagger).$$

The generated state is a centered Gaussian state $|\Phi(r)\rangle$ which we call the two-mode squeezed state with parameter r. Its representation in the number basis is given by

$$|\Phi(r)\rangle = \frac{1}{\cosh(r)} \sum_{n=0}^{\infty} \tanh^n(r)|n\rangle|n\rangle. \tag{32}$$

The covariance matrix of the two-mode squeezed state is given by

$$\gamma_{2mode} = \begin{pmatrix} \cosh 2r\, \mathbb{1} & \sinh 2r\sigma_z \\ \sinh 2r\sigma_z & \cosh 2r\, \mathbb{1} \end{pmatrix}$$

where $\sigma_z = \begin{pmatrix} 1 & 0 \\ 0 & -1 \end{pmatrix}$.

To illustrate the properties of the state $|\Phi(r)\rangle$ a little more, the observation of the x quadrature on one of the modes is equivalent to the projection of the state $|x'\rangle$ on one mode of the squeezed state. This case is covered by Lemma 3.3 and yields for the x quadrature of the untouched mode

$$\tilde{x} = x_1 + (x' - x_2)\frac{\sinh 2r}{\cosh 2r}$$

37

which goes to $\tilde{x} = (x_1 - x_2) + x'$ in the limit of perfect squeezing $r \to \infty$ (perfect entanglement). If the initial displacement of the two mode squeezed state vanishes, then the mode that was not measured exhibits the same quadrature as the mode that was measured.

4 Quantum teleportation

Quantum teleportation is an impressive primitive of quantum information processing; it allows two people to communicate quantum information by using shared entanglement and classical communication only. This section will go over the details of the procedure to transmit (teleport) a quantum state, both in the finite-dimensional case and the infinite-dimensional case.

4.1 Finite-dimensional systems

For simplicity, we will only cover the protocol for qubits, but it is possible to generalize it to the teleportation of qudits using the same ideas. Suppose Alice and Bob share a Bell state $|\Phi_2^+\rangle$ and Alice would like to transfer an arbitrary state $|\psi\rangle = \alpha|0\rangle + \beta|1\rangle$ to Bob. The protocol for quantum teleportation proceeds as follows [11], see Figure 2.

Protocol 4.1: Quantum teleportation of qubits

Input: maximally entangled state $|\Phi_2^+\rangle$ and arbitrary quantum state $|\psi\rangle$. Output: $|\psi\rangle$ at another location.

1. Alice does a Bell measurement on the qubit she has to teleport and her half of the Bell state. She obtains some classical result.

2. Alice sends that classical information to Bob via a classical channel.

3. Bob receives the outcome and depending on it, applies a conditional operation on his half of the Bell state.
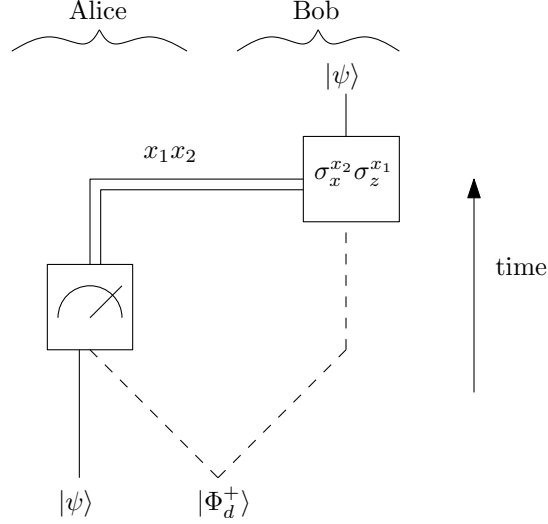
Figure 2: A schematic representation of the teleportation Protocol 4.1. The dotted line represents entanglement between two systems. The time flow is upward.

After the last step, Bob has in his possession a perfect copy of the state Alice wanted to teleport. More specifically, the state of the whole system $|S\rangle$ before the protocol starts is

$$|S\rangle = |\psi\rangle|\Phi_2^+\rangle = (\alpha|0\rangle + \beta|1\rangle)\frac{1}{\sqrt{2}}(|00\rangle + |11\rangle) = \frac{1}{\sqrt{2}}(\alpha|000\rangle + \alpha|011\rangle + \beta|100\rangle + \beta|111\rangle)$$

$$= \frac{1}{2}(|\Phi_2^+\rangle(\alpha|0\rangle + \beta|1\rangle) + |\Phi_2^-\rangle(\alpha|0\rangle - \beta|1\rangle) + |\Psi_2^+\rangle(\beta|0\rangle + \alpha|1\rangle) + |\Psi_2^-\rangle(\beta|0\rangle - \alpha|1\rangle))$$

where the last expression was obtained via the following,

$$|00\rangle = \frac{1}{\sqrt{2}}(|\Phi_2^+\rangle + |\Phi_2^-\rangle)$$

$$|11\rangle = \frac{1}{\sqrt{2}}(|\Phi_2^+\rangle - |\Phi_2^-\rangle)$$

$$|01\rangle = \frac{1}{\sqrt{2}}(|\Psi_2^+\rangle + |\Psi_2^-\rangle)$$

$$|10\rangle = \frac{1}{\sqrt{2}}(|\Psi_2^+\rangle - |\Psi_2^-\rangle).$$

39

Now if Alice does a measurement in the Bell basis, Bob's part of the state will collapse to one of the combinations $\alpha|0\rangle + \beta|1\rangle$, $\alpha|0\rangle - \beta|1\rangle$, $\beta|0\rangle + \alpha|1\rangle$ or $\beta|0\rangle - \alpha|1\rangle$, each containing all the information about the state $|\psi\rangle$. Bob does not know *which* combination he has. This is what prevents this protocol from doing any faster-than-light communication. Calculating the mixture Bob has without any information of Alice's measurement indicates that he has a completely mixed state so he cannot infer any information about the input state. He still needs Alice's two bits of classical information to know what transformation to apply to recover $|\psi\rangle$, the Not gate (σ_x) and/or Phase Flip gate σ_z or just the identity operation.

Note also that in every case, the state is *perfectly* teleported every time. The fidelity of quantum teleportation is always 1, independently of the input state. For this reason, the fidelity averaged over input states or Alice's measurement is also 1 in any case. This result stays true if the input is not a pure state. This is because the teleportation map is a linear map. Since any mixed state can be decomposed as a mixture of pure states $\rho = \sum_i p_i |\psi_i\rangle\langle\psi_i|$ and each one is teleported perfectly, Bob obtains ρ without distortion.

4.2   Infinite-dimensional systems

This protocol can be extended to continuous variables systems. We will call the resulting scheme the Vaidman-Braunstein-Kimble Protocol [25, 26]. The main ideas for the procedure are identical. Let us discuss the resources we need in the infinite-dimensional case.

First, entanglement is required to teleport a quantum system. In the finite-dimensional case it was provided by a Bell state whereas in infinite-dimensional setting, entanglement is supplied in the form of a two-mode squeezed state. Secondly, we needed to be able to do a Bell measurement. When working with qubits, a Bell measurement is accomplished by a CNOT gate and then a Hadamard gate on the control wire before measuring both qubits in the computational basis. We have established earlier in Section 3.5 that the analogue of the CNOT as the entangling gate is

given by the 50:50 beam-splitter. The Hadamard gate is necessary so it is possible to distinguish states in the bases $\{|0\rangle, |1\rangle\}$ and $\{\frac{1}{\sqrt{2}}(|0\rangle \pm |1\rangle)\}$ respectively. Seeing that each element in the first basis is a superposition of the elements in the second basis, we can associate each basis with either quadrature x or p. Since localized x implies delocalized p and vice versa, this is analogous to the finite-dimensional case. Therefore, we need to be able to do measurements of the x and p quadratures, i.e. homodyne measurement.

4.2.1 The Vaidman-Braunstein-Kimble protocol

Here is the protocol used by Alice and Bob (see Figure 3). It uses three modes which we index by $1, 2, 3$; we also indicate by A and B who the mode belongs to.

Protocol 4.2: Vaidman-Braunstein-Kimble protocol

Input: Two-mode squeezed state $|\Phi(r)\rangle_{A_2 B_1}$ shared between Alice and Bob (i.e., on modes 1 and 2). One-mode unknown quantum state $|\Psi\rangle_{A_3}$ for Alice. Output: Quantum state $|\Psi'\rangle_{B_1}$ on Bob's side

1. Alice combines the two modes (one from the two-mode squeezed state and one from the unknown quantum state) in her possession with a beam-splitter.

2. Alice performs homodyne measurement on her two modes, x on one mode and p on the other one which produces the classical outcome (x_c, p_c).

3. Alice transmits to Bob the outcome via classical communication.

4. Bob displaces his mode by $\sqrt{2}x_c$ and $\sqrt{2}p_c$ in the x and p direction respectively. The resulting state is the output state $|\Psi'\rangle$.

41

4.2.2 Analysis assuming perfect entanglement

In the limit $r \to \infty$ of infinite squeezing, the analysis of the Vaidman-Braunstein-Kimble protocol is especially simple. We can analyze it in the Heisenberg picture. Suppose Alice wants to teleport mode 3 while having mode 2 from the two-mode squeezed state, leaving Bob with mode 1. Since it is an EPR pair, the quadratures are correlated: $x_1 - x_2 = 0$ and $p_1 + p_2 = 0$. Alice first uses the beam-splitter which creates the new modes

$$x_2' = \frac{x_2 + x_3}{\sqrt{2}} \qquad \text{and} \qquad p_2' = \frac{p_2 + p_3}{\sqrt{2}}$$
$$x_3' = \frac{-x_2 + x_3}{\sqrt{2}} \qquad \text{and} \qquad p_3' = \frac{-p_2 + p_3}{\sqrt{2}}$$

and then she measures $p = \frac{p_2 + p_3}{\sqrt{2}}$ on mode 2 and $x = \frac{-x_2 + x_3}{\sqrt{2}}$ on mode 3. Because of the properties of the EPR pair, the measurement has the following effect on Bob's modes

$$x_1'' = x_3 - \sqrt{2}x \qquad \text{and} \qquad p_1'' = p_3 - \sqrt{2}p.$$

Then Bob displacing his mode by $\sqrt{2}(x, p)$ will complete the teleportation as his mode is identical to mode 3 that was to be teleported.

4.2.3 Analysis assuming imperfect entanglement

In practice, the squeezing r of the resource state $|\Phi(r)\rangle$ is finite. Here we discuss how this affects the quality of teleportation: the amount of squeezing available will determine how close Bob's final state is to the one Alice tried to teleport. Their resource is now the two-mode squeezed state $|\Phi(r)\rangle$ rather than a perfect EPR pair. The idea for the mathematical demonstration is the same, except that we have the following relation for the EPR pair $x_1 - x_2 = \sqrt{2}e^{-r}x_2^0$ and $p_1 + p_2 = \sqrt{2}e^{-r}p_1^0$. Here the superscript 0 indicates the modes of independent states before being entangled. Using
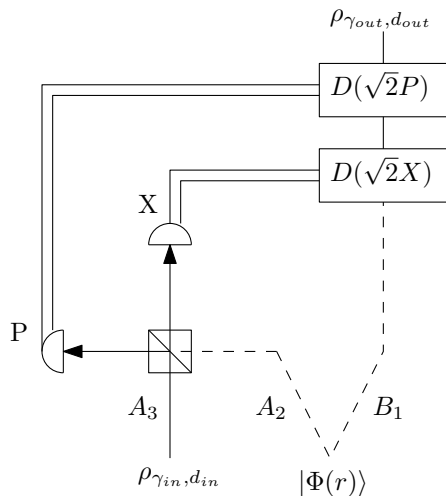
Figure 3: This is the Vaidman-Braunstein-Kimble Protocol 4.2 for teleportation of continuous variables. The input is an arbitrary state with covariance matrix γ_{in} and displacement d_{in}. The half circles represent homodyne detection. The hashed box is a 50:50 beamsplitter. Bob has mode B_1 from the two-mode squeezed state while Alice has mode A_2 from the two-mode squeezed state and mode A_3 from the unknown state.

these relations means that Bob will have the following modes after displacement

$$x_1'' = x_3 + e^{-r}x_2^0 \qquad \text{and} \qquad p_1'' = p_3 + e^{-r}p_1^0.$$

From this, it is evident that imperfect squeezing will introduce noise in the teleported modes.

The Heisenberg picture offers a simple way to demonstrate how quantum teleportation works using continuous variables but it is useful to have a description of the protocol in phase space. The Heisenberg picture gives information about the mean values of operators where in many cases it may be necessary to have information about, say, the fidelity for the teleportation of a given state.

In Appendix C, we give a description and analyze teleportation in terms of characteristic functions. In particular, we show that when teleporting a Gaussian state $|\Psi\rangle$, the teleported state $|\Psi'\rangle$ is also Gaussian. We also compute the covariance matrix γ_{out} and the displacement d_{out} of $|\Psi'\rangle$ as a function of γ_{in}, d_{in} (the covariance matrix and the displacement of $|\Psi\rangle$) and the squeezing param-

eter r of the resource state. The calculation is based on Lemma 3.4 to compute the characteristic function at the output averaged over the results of homodyne detection. Because of the imperfect squeezing in the resource, the final state will depend on the values obtained for the homodyne measurement.

4.3 Teleportation of coherent states

Assuming we want to teleport $|\alpha\rangle$ (which has displacement and covariance matrix given by (23)), we can specialize the result of appendix C ($a = d = 1$, $b = c = 0$ for Lemma C.1) and show that the output state is a thermal state (see (60)).

One important quantity that can be calculated is the fidelity averaged over the measurement results (see also Appendix C). From the results in appendix D, the fidelity of two Gaussian states (covariance matrices γ_i and displacements d_i, $i = 1, 2$) when one of them is pure is given by (61)

$$F = \frac{2 \exp\left(-(d_1 - d_2)^T (\gamma_1 + \gamma_2)^{-1} (d_1 - d_2)\right)}{\sqrt{\det(\gamma_1 + \gamma_2)}}. \tag{33}$$

Therefore the fidelity between the two Gaussian states (one of them being pure) with identical displacement and covariance matrices γ_{in} and γ_{out} can be written as

$$F = \frac{2}{\sqrt{\det(\gamma_{in} + \gamma_{out})}}. \tag{34}$$

Calculating the fidelity of the teleportation map $\mathcal{T}$ applied to a coherent state $|\alpha\rangle$ gives us

$$F(\mathcal{T}, |\alpha\rangle) = \frac{1}{1 + e^{-2r}}.$$

This fidelity is interesting because it does not depend on the initial coherent state we wanted to teleport, therefore this formula is valid for any coherent state $|\alpha\rangle$. It can also be seen that in the

limit of infinite squeezing, $r \to \infty$, we obtain unit fidelity as expected.

4.4 Benchmark

We want to be sure that our quantum strategies will be better than what could be done without entanglement. This brings us to the subject of benchmarks quantum teleportation has to surpass in order to beat any such strategy. There are different criteria to check to establish this and they usually depend on which class of states we try to teleport. For instance, Horodecki et al [16] found the fidelity a teleportation process has to beat in order to surpass any measure and prepare scheme (Alice measures the input state to obtain as much information as possible about the state and sends the classical information to Bob who uses this knowledge to prepare a copy of that state) to transmit a quantum state distributed according to the uniform Haar measure over $\mathbb{C}^d$,

$$\bar{F}_{benchmark} = \frac{2}{d+1}. \tag{35}$$

The best strategy Alice and Bob can do to send a coherent state without entanglement (as quantum communication) is a measure and prepare protocol. Chiribella and Xie [23] developed a benchmark for the case of amplification of coherent states (taking $|\alpha\rangle$ to $|g\alpha\rangle$ where g is the amplification gain) with Gaussian prior $p_\lambda(\alpha) = \frac{\lambda}{\pi} e^{-\lambda |\alpha|^2}$ for a general quantum map. Specializing to teleportation ($g = 1$), it implies that the optimal average fidelity achievable by means of local quantum operations and classical communication without entanglement (i.e. a measure and prepare protocol) is given by $\bar{F} = \frac{\lambda+1}{\lambda+2}$. Therefore, given enough squeezing for the EPR pair, the fidelity for teleportation of a coherent state is always be better than the classical case.

5 Port-based teleportation

Port-based teleportation is different from the previously studied "standard" quantum teleportation. This time Bob has N outputs ports and he gets the quantum state Alice wants to send him by selecting one of the N ports, this choice depending on the outcome of Alice's measurement. This protocol is useful for applications because Bob does not need to apply any transformation on his system, he only needs to pick the right port to find the teleported state. This advantage comes with a cost, the protocol succeeds with unit fidelity only in the limit of infinite entanglement, even in the finite-dimensional case.

5.1 Protocol

The execution of the protocol is similar in spirit to what is done for standard quantum teleportation. Assume Alice and Bob share N Bell states (every qudit from these Bell states is called a port) $|\Phi_d^+\rangle_{AB} = \frac{1}{\sqrt{d}} \sum_i |i\rangle_{A_i} |i\rangle_{B_i}$ and Alice has to teleport a state $|\psi\rangle_S$. Here $A = \cup_i A_i$ and similarly for Bob. The procedure is as follows

---

Protocol 5.1: Port-based teleportation

Input: arbitrary quantum state $|\psi\rangle_S$ to be teleported. Shared resource state entanglement $|\Phi_d^+\rangle_{AB}$ Output: quantum state $|\psi'\rangle_S$ close to $|\psi\rangle_S$

1. Alice does a measurement on SA by performing some POVM $\{E_i\}$ and obtains outcome $i \in \{1, ..., N\}$. She sends the index i to Bob

2. Bob discards every port except for the ith one, which is mathematically equivalent to tracing out $\bar{B}_i = B \backslash B_i$. No further action is required by Bob.

After the last step, Bob has in his possession a state $|\psi'\rangle$ close to the state $|\psi\rangle$. Mathematically speaking, the port-based teleportation CPTP map can be written as (in what follows, $|\psi\rangle\langle\psi|$ is

Figure 4: A schematic representation of Protocol 5.1. Alice has system SA while Bob has system B and S' for the output.

written as ψ for brevity and $\bar{B}_i$ stands for $B \backslash B_i$)

$$\mathcal{T}(\rho_S) = \sum_i \mathsf{tr}_{SA\bar{B}_i} \left[(E_{SA}^i \otimes \mathbb{1}_B)(\rho_S \otimes \Phi_{AB}^{\otimes N}) \right].$$

We wish to learn how close the input and the output given by this map are. To do this, we will use a different formulation of the problem in the next section.

5.2   Relation to distinguishability

The study of the port-based teleportation map is in general complicated as we do not yet know what the POVM $\{E_i\}$ looks like. Our goal is to maximize the fidelity of this map by choosing a good POVM. We relate this task to our ability to distinguish ensembles of quantum states which is a better understood and more conventional problem.

We give a statement that can be used both for finite and infinite-dimensional systems and that can also be used either for the average fidelity or for the entanglement fidelity. Such statements

47

already existed for specific cases but our contribution provides a single relation that is valid in more general cases. This way we are able to recover the known results in finite dimension (see Corollary 5.2). For this reason, we will cast our results in terms of a more general quantity which we will call the general fidelity f of the map $\mathcal{T}$,

$$f(\mathcal{T}, |\psi_\alpha\rangle, dp(\alpha)) := \int dp(\alpha) \langle \psi_\alpha |_{DS'} (\mathbb{I}_D \otimes \mathcal{T}_S)(\psi_{DS}^\alpha) |\psi_\alpha\rangle_{DS'} \tag{36}$$

for a given ensemble of state $\{dp(\alpha), |\psi_\alpha\rangle_{DS}\}$ with probability measure $dp(\alpha)$. We introduced a reference system D to be able to express the entanglement fidelity with this relation by using $|\psi_\alpha\rangle_{DS} = |\Phi_d^+\rangle_{DS}$ for all α. Since the maximally entangled state does not depend on the parameter α, the probability distribution can be arbitrary. The integral and the probability distribution will cancel out. In general, one can take an input state $|\psi\rangle_{DS}$ that does not depend on α if we do not want an average fidelity. On the other hand, if we do not want to calculate the fidelity on a bipartie state, we can define the input as a tensor product of two normalized pure states $|\psi_\alpha\rangle_{DS} = |\phi\rangle_D |\psi_\alpha'\rangle_S$ where $|\phi\rangle$ is arbitrary. Since the map $\mathbb{I}_D \otimes \mathcal{T}_S$ acts only on S, the D systems will be projected onto each other and cancel out. Therefore, we can use equation (36) to treat the fidelities of the teleportation map in full generality.

The relation between port-based teleportation and hypothesis testing is then given by the following theorem.

Theorem 5.1 (Port-based teleportation and hypothesis testing) *Assume that Alice and Bob share $\Phi_{AB}^{\otimes N}$, where $|\Phi\rangle_{AB}$ is a bipartite entangled resource state. Consider the port-based teleportation protocol 5.1 for teleporting a state on S (at Alice's side) to a system $S' \cong B$ (at Bob's side). Let $\mathcal{T} : \mathcal{B}(S) \to \mathcal{B}(S')$ be the corresponding CPTP map, that is,*

$$\mathcal{T}(\rho_S) = \sum_i \mathsf{tr}_{SA\bar{B}_i} \left[(E_{SA}^i \otimes \mathbb{1}_B) \left(\rho_S \otimes \Phi_{AB}^{\otimes N} \right) \right] ,$$

where $\{E_{SA}^i\}_{i=1}^N$ is some fixed POVM. Assume that Alice wants to teleport system S from an ensemble $\{dp(\alpha), |\psi_\alpha\rangle_{DS}\}$ of bipartite pure states characterized by the continuous parameter α (here dp is a probability measure). Then the general fidelity (36) can be expressed as

$$f(\mathcal{T}, |\psi_\alpha\rangle, dp(\alpha)) = CNp_{succ},$$

where $p_{succ} = \frac{1}{N}\sum_i E_i\rho_i$ is the probability of successfully distinguishing the states

$$\rho_i = \frac{1}{C}\left[\int dp(\alpha)q_\alpha\theta_{SA_i}^\alpha\right] \otimes \tau_{\bar{A}_i}^{\otimes(N-1)}$$

using the POVM $\{E_{SA}^i\}_{i=1}^N$. The different terms in this expression of ρ_i are defined as

$$C = \int dp(\beta)q_\beta,$$

that is, a normalization factor for the states to distinguish,

$$\tau_{A_i} = \mathsf{tr}_B\Phi_{A_iB},$$

the reduced density operator of the resource state and finally $\theta_{SA_i}^\alpha$, the projector onto the state

$$|\theta_\alpha\rangle_{SA_i} = \frac{1}{\sqrt{q_\alpha}}(\mathbb{1}_{SA_i} \otimes \langle\psi_\alpha|_{DB_i})|\psi_\alpha\rangle_{DS}|\Phi\rangle_{A_iB_i}. \tag{37}$$

Proof The overlap occurring in the expression of the general fidelity can be written as the trace

over the projector. This trace combined with the discarding operation of Bob reads

$$\langle\psi_\alpha|(\mathbb{I}\otimes\mathcal{T})(\psi_\alpha)|\psi_\alpha\rangle = \sum_i \mathsf{tr}_{DSAB}\left((\psi^\alpha_{DB_i}\otimes\mathbb{1}_{SA\bar{B}_i})\left[(E^i_{SA}\otimes\mathbb{1}_{DB})\left(\psi^\alpha_{DS}\otimes\Phi^{\otimes N}_{AB}\right)\right]\right)$$

$$= \sum_i \mathsf{tr}_{SA}\left(E^i_{SA}\mathsf{tr}_{DB}\left[(\psi^\alpha_{DB_i}\otimes\mathbb{1}_{SA\bar{B}_i})(\psi^\alpha_{DS}\otimes\Phi^{\otimes N}_{AB})\right]\right).$$

It is straightforward to compute the trace over the system $\bar{B}_i$

$$\mathsf{tr}_{DB}\left[(\psi^\alpha_{DB_i}\otimes\mathbb{1}_{SA\bar{B}_i})(\psi^\alpha_{DS}\otimes\Phi^{\otimes N}_{AB})\right] = \tau^{\otimes(N-1)}_{\bar{A}_i}\otimes\mathsf{tr}_{DB_i}\left[(\psi^\alpha_{DB_i}\otimes\mathbb{1}_{SA_i})(\psi^\alpha_{DS}\otimes\Phi_{A_iB_i})\right].$$

The last part of this expression is defined on system SA_i and can be related to the definitions given in the statement of the lemma

$$q_\alpha\theta^\alpha_{SA_i} = \mathsf{tr}_{DB_i}\left[(\psi^\alpha_{DB_i}\otimes\mathbb{1}_{SA_i})(\psi^\alpha_{DS}\otimes\Phi_{A_iB_i})\right]$$

where the constant q_α is necessary since the projection produces an unnormalized state. Getting all these terms back into the expression for the general fidelity yields

$$f(\mathcal{T},|\psi_\alpha\rangle, dp(\alpha)) = \int dp(\alpha)\sum_i \mathsf{tr}\left(E^i_{SA}\left[q_\alpha\theta^\alpha_{SA_i}\otimes\tau^{\otimes(N-1)}_{\bar{A}_i}\right]\right)$$

$$= N\int dp(\beta)q_\beta\frac{1}{N}\sum_i\mathsf{tr}\left(E^i_{SA}\left[\frac{\int dp(\alpha)q_\alpha\theta^\alpha_{SA_i}}{\int dp(\beta)q_\beta}\otimes\tau^{\otimes(N-1)}_{\bar{A}_i}\right]\right)$$

and the claim follows. ∎

As an application of the last theorem, we reproduce the result from [17] stating that entanglement fidelity is related to the quantum hypothesis testing problem for finite-dimensional systems.

Corollary 5.2 (Equivalent hypothesis testing problem in finite dimension) *The entanglement fidelity $F_{ent}(\mathcal{T},|\Phi^+_d\rangle)$ of the port-based teleportation channel $\mathcal{T}:\mathbb{C}^d\to\mathbb{C}^d$ with N ports and*

resource state $|\Phi_d^+\rangle = \frac{1}{\sqrt{d}} \sum_{i=0}^{d-1} |i\rangle|i\rangle$ is given by

$$F_{ent}(\mathcal{T}, |\Phi_d^+\rangle) = \frac{N}{d^2} p_{succ}$$

where p_{succ} is the probability of successfully distinguishing between the states

$$\rho_i = \Phi_{SA_i} \otimes (\mathbb{1}/d)_{\bar{A}_i}^{\otimes(N-1)}.$$

Proof We are going to use the results from theorem 5.1 to prove this corollary. We need to compute τ, θ and C and the result will follow. First

$$\tau = \text{tr}_B(\Phi_{AB}) = \frac{1}{d} \sum_{nop} (\mathbb{1}_A \otimes \langle n|_B)|oo\rangle\langle pp|_{AB}(\mathbb{1}_A \otimes |n\rangle_B)$$

$$= \frac{1}{d} \sum_{nop} \delta_{no}\delta_{pn}|o\rangle\langle p|_A = \frac{1}{d} \sum_n |n\rangle\langle n|_A = \frac{\mathbb{1}_A}{d}$$

which is the maximally mixed state. For θ

$$|\theta\rangle_{SA_i} = \frac{1}{\sqrt{q}}(\mathbb{1}_{SA_i} \otimes \langle\Phi^+|_{DB_i})|\Phi_d^+\rangle_{DS}|\Phi_d^+\rangle_{A_iB_i}$$

$$= \frac{1}{\sqrt{d^3q}} \sum_{nop} (\mathbb{1}_{A_i} \otimes \langle nn|_{DB_i})|oo\rangle_{DS}|pp\rangle_{A_iB_i}$$

$$= \frac{1}{\sqrt{d^3q}} \sum_{nop} \delta_{no}\delta_{pn}|o\rangle_S|p\rangle_{A_i} = \frac{1}{\sqrt{d^3q}} \sum_n |nn\rangle_{SA_i} = \frac{1}{\sqrt{d^2q}}|\Phi_d^+\rangle_{SA_i}$$

and we see that for the state to be normalized we need $q = \frac{1}{d^2}$ which means

$$C = \frac{1}{d^2}.$$

∎

51
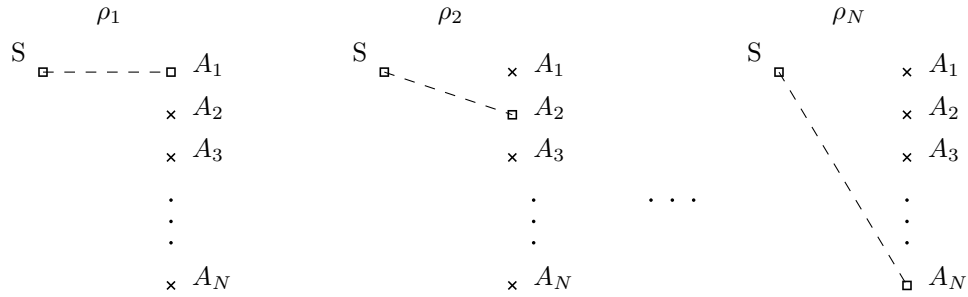
Figure 5: A representation of the states to distinguish in the ensemble specified by the Corollary 5.2. Again, the dashed line is used to represent entanglement between two systems (the squares), system S and one of the A_i's. The cross represents a maximally mixed state.

The states to be distinguished in the last corollary have a simple form. The system SA is defined on $N + 1$ ports, $N - 1$ of them are described by the maximally mixed state and the last two ports are maximally entangled. The entanglement is always between S and one of the N other port (one of the A_i's), our task is to find to which port it is entangled to. See Figure 5.

In the case of teleportation channels, Horodecki et al [16] found that for finite-dimensional systems, there is a one-to-one relation between the average fidelity $\bar{F}$ over uniformly distributed input states of dimension d and the entanglement fidelity F_{ent}

$$\bar{F} = \frac{F_{ent}d + 1}{d + 1}. \tag{38}$$

Therefore the measurement that maximizes the entanglement fidelity will also maximize the average fidelity. The result of Corollary 5.2 then tells us what the average fidelity is for the teleportation of a state from the Haar uniform ensemble over $\mathbb{C}^d$,

$$\bar{F} = \frac{Np_{succ}/d + 1}{d + 1}.$$

52

5.3 Lower bound

We are now trying to find the optimal probability of success of distinguishing the ensemble of states described in Figure 5. However, if we can find a lower bound on this probability of success saying that we can distinguish quantum states *well enough* we would also be satisfied. Therefore if we find a measurement with high enough probability of success, we can say that port-based teleportation is a viable protocol for the transmission of quantum information. It turns out that the PGM satisfies this requirement. This comes from a lower bound on the PGM itself found by Beigi and Koenig [17]

$$p_{succ}^{PGM} \geq \frac{1}{N\bar{r}\mathsf{tr}\bar{\rho}^2}$$

where $\bar{r} = \frac{1}{N}\sum_i \mathrm{rank}(\rho_i)$ is the average rank and in the same fashion $\bar{\rho} = \frac{1}{N}\sum_i \rho_i$ is the average of the states to distinguish. We carried the calculations for these quantities in appendix E. The resulting entanglement fidelity is

$$F_{ent}(\mathcal{T},|\Phi_d^+\rangle) \geq 1 - \frac{d^2-1}{N} \geq 1 - \frac{d^2}{N} \tag{39}$$

and for the average fidelity we get with (38)

$$\bar{F}(\mathcal{T}) \geq 1 - \frac{d(d-1)}{N} \geq 1 - \frac{d^2}{N}.$$

In both cases, the fidelity goes to 1 when the number of port is infinite ($N \to \infty$). Although it might require a huge amount of entanglement as a port is synonymous to an EPR pair, it is at least possible to use port-based teleportation in principle. Using the bound found by Horodecki et al (see (35)), we see that in order to have $\bar{F} \geq \bar{F}_{benchmark}$, we need $N \geq d(d+1)$. We need at most $\sim d^2$ e-dits of entanglement.

Beigi and Koenig [17] add an interesting perspective on the possibility of having high entanglement fidelity for the teleportation map. They could relate (39) to a statement about how close the teleportation map $\mathcal{T}$ is to the identity channel $\mathbb{I}$ by using (8) which leads to

$$\|\mathcal{T} - \mathbb{I}\|_\diamond \leq \frac{4d^2}{\sqrt{N}}. \tag{40}$$

Since a norm on superoperators (like the diamond norm) is related to the maximum of the norm defined over a normalized input set, the diamond norm is a measure of how close two quantum channels are in the worst case scenario. This statement presents the advantage of being independent of the input state, which is not the case for say the average fidelity.

5.4   Qubit case

Ishizaka and Hiroshima [18, 19] studied this teleportation scheme in great detail for the qubit case $(d = 2)$ to compute the entanglement and average fidelity. The strategy was to use the relation between qubits and 1/2 spins as basis of $SU(2)$ to diagonalize the operator $\sum_i \rho_i$ i.e. the average of the states to distinguish. Based on those calculations, it was possible to use a semidefinite program to compute the optimal measurement to the distinguishability problem. Moreover, Ishizaka and Hiroshima covered different variations of the protocol. There is a deterministic protocol that is always successful but with imperfect fidelity and a probabilistic protocol that only succeeds part of time but when it does, it is with unit fidelity. Furthermore, we can make a distinction between maximally entangled resource states and optimal resource states.

In the deterministic case for a maximally entangled state, the average fidelity behaves in the limit of $N \to \infty$ as

$$\bar{F}(\mathcal{T}) \to 1 - \frac{1}{2N}$$

and it is obtained by performing the PGM. In this case ($d = 2$), we need $\bar{F} \geq \frac{2}{3}$ to have something better than the optimal measure and prepare scheme (cf. (35)). The result given by Ishizaka and Hiroshima indicates that we need $N \geq 3$ for this condition to be fulfilled.

For an optimal resource state

$$\bar{F}(\mathcal{T}) \rightarrow \frac{2}{3} + \frac{1}{3} \cos \frac{2\pi}{N+2}$$

but the measurement is different from the PGM.

For the probabilistic case, the figure of merit is of course the probability of success, which is given by

$$p \rightarrow 1 - \sqrt{\frac{8}{\pi N}}$$

for a maximally entangled state and

$$p \rightarrow 1 - \frac{3}{N+3}$$

if the resource is optimal as well.

5.5   Port-based superdense coding

Superdense coding is a way to enhance classical communication by using entanglement and quantum communication. Interestingly, every teleportation protocol can be related to a superdense coding scheme [24]. This involves exchanging the operations of the sender and the receiver. For instance, with standard teleportation, Alice applies a Pauli gate on a qubit of an entangled state she previously shared with Bob. She performs the transformation according to the classical information she wants to send and then sends her qubit to Bob. He then does a Bell measurement to retrieve the classical
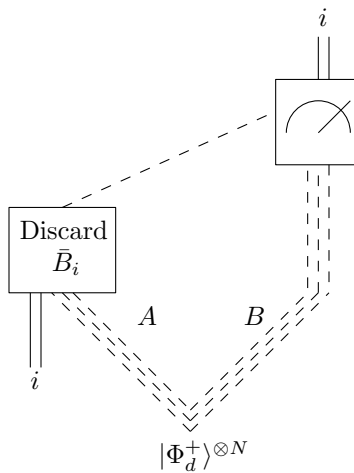
Figure 6: This figure illustrates the idea behind port-based superdense coding (Protocol 5.2). It is essentially the same as for port-based teleportation with the measurement boxes exchanged.

index which constitutes the message Alice wanted to send. This way, Alice can transmit two classical bits of information, using only 1 bit of quantum communication and 1 EPR pair.

Here we show that the same is true for port-based teleportation, which had never been done before. We call the resulting scheme port-based superdense coding. The protocol goes as follows (see Figure 6).

Protocol 5.2: Port-based superdense coding

Input: N maximally entangled states $|\Phi_d^+\rangle$ shared between Alice and Bob. Classical index $i \in \{1, ..., N\}$ for Alice to send. Output: classical index for Bob

1. Alice sends one of the N ports to Bob. The index i of this port is the classical information Alice wants to transmit.

2. Bob applies the measurement specified in the distinguishing problem for port-based teleportation (see Section 5.3). The outcome of this measurement is Bob's estimate of the message Alice wanted to send.

It is easy to see why this protocol works. When Alice sends one of her ports to Bob, his task his basically to figure out to which of his ports the input is entangled to. This is exactly the distinguishing problem mentioned for the calculation of the entanglement fidelity, therefore the probability of Bob successfully getting Alice's message is given by p_{succ} in Appendix E.

At first it might seem that we would be able to send an arbitrary amount of classical information as long as we have enough entanglement to "support" this message. But because the size of our alphabet depends on N and $p_{succ} \sim \frac{d^2}{N}$ (cf. (62) in Appendix E), there is a trade off between the quantity of information we can send and the chances of correctly interpreting the message. That is, in port-based superdense coding, 1 qudit of communication boosts the success probability from $1/N$ (random guessing without communication) to d^2/N. In this case the measurement is used for decoding whereas in the teleportation protocol it is used to collapse Bob's resources to a quantum state similar to the input state. For teleportation, the outcome of Alice's measurement is not important, what matters is how it influences the quality of the state on Bob's side.

5.6 Applications of port-based teleportation

Quantum teleportation is of course an interesting feature in itself for the transmission of quantum information but it can also be used for various applications. We will discuss some of them here and mention how port-based teleportation offers advantages over standard quantum teleportation. Port-based teleportation might not seem interesting as it requires a large amount of entanglement for an output state with imperfect fidelity, but these drawbacks are compensated by the simplicity of Bob's conditional operation.

5.6.1 Universal programmable quantum processor

The idea of a universal quantum processor is that you can store and retrieve an arbitrary operation in a quantum state so you can use it whenever you want. Quantum teleportation does so by taking

advantage of the following property or the maximally entangled state $|\Phi_d^+\rangle$

$$(U \otimes \mathbb{1})\, |\Phi_d^+\rangle = \left(\mathbb{1} \otimes U^T\right) |\Phi_d^+\rangle.$$

Applying a transformation on one qubit of an EPR pair is the same as applying the transpose of that same unitary but on the other qubit. Then, using the port-based teleportation protocol and applying U^T on Alice's half of each EPR pair before she does her measurement will produce the output $U|\psi\rangle$ on Bob's port. This would be more complicated with standard quantum teleportation. Because of the correction Bob needs to apply, the output state is given by $U\sigma_i|\psi\rangle$. The operation is successful only if the correction to apply is the identity or the unitary U commutes with the Pauli matrices. We can use the same idea to apply arbitrary quantum operations $\mathcal{E}$ by storing them in Bob's half of the EPR pair.

Assuming we can store quantum states and easily generate entanglement, we can apply a transformation on an EPR pair, store it until we need to use it and then do port-based teleportation to apply the transformation on some arbitrary input state.

5.6.2 Instantaneous non-local computations

This application is based on Vaidman's recursive scheme [31] for instantaneous computation which takes advantage of the fact that once the measurement is done in the protocol, Bob's half of the system has already collapsed to a state that is closely related to the input. It might then be possible to act on this output before getting the classical information. This is complicated for standard teleportation because of the σ_i transformation that comes with the output, but this is not a problem with port based teleportation.

The goal of non-local computations is for two separated protagonists, Alice and Bob, to each receive one half of a bipartite state and apply some non-local operation on that state. This non-local operation is such that it cannot be expressed as a tensor product on two Hilbert spaces and we

want this task to be done with only one round of classical communication. This seems impossible as Alice and Bob would at least need to be able to freely communicate with each other to apply this transformation. What we mean by instantaneous is that Alice's and Bob's operations are not conditioned on classical communication until the very end of the protocol. Also, we assume the time of local operations is negligible compared to the time required for classical information to reach its destination.

Here we show how to do this with quantum teleportation and one round of classical communication with an arbitrary good fidelity depending on how well we can use port-based teleportation. Although Bob never knows on which port the state was teleported right after Alice's measurement, it is nonetheless possible to act on it. The protocol proceeds as follows [17]

Protocol 5.3: Instantaneous non-local computation

Input: information on the unitary U_{AB} Alice and Bob want to implement and the bipartite state ρ_{AB}. Output: a bipartite state close to $U_{AB}\rho_{AB}U_{AB}^{\dagger}$.

1. Bob performs standard teleportation (here teleportation should be understood as the measurement without sending the classical information as we want to keep things instantaneous) for his input. Alice has now in her possession $(\mathbb{1} \otimes \sigma_b)|\psi\rangle$ for $b \in \{0,1,2,3\}^n$.

2. Alice teleports back the state to Bob, using port-based teleportation this time. Bob now has the state $(\mathbb{1} \otimes \sigma_b)|\psi\rangle$ for $b \in \{0,1,2,3\}^n$ with high fidelity on one of his N ports (number of ports he and Alice agreed on previously), although he does not know which one.

3. Bob, knowing what index he got for the first teleportation, applies the transformation $U(\mathbb{1} \otimes \sigma_b)$ on each of his ports.

4. At this point the operation is already successful, Bob applied the desired transformation. Assuming we want Alice and Bob to have one half of the system at the end of protocol as in the initial setup of the problem, Bob uses standard teleportation to send one half from each of his N ports to Alice. She now gets $(\sigma_{b_i} \otimes \mathbb{1})|\psi\rangle$ for $\forall i \in \{1, ..., N\}$.

5. Alice sends to Bob the information about which port the system was in after port-based teleportation and Bob uses this information to discard all the ports except for the specified port. Bob sends to Alice what correction should be applied on each of the N ports that was sent, she keeps the only relevant port on which she applies the correction σ_{b_i}.

Once again, standard quantum teleportation would not have been as useful since both Alice and Bob would need to apply corrections after each teleportation round. In fact, using port-based

$$U_{AB}\rho_{AB}U_{AB}^{\dagger}$$
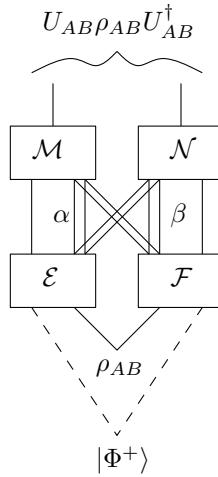
Figure 7: This figure illustrates Protocol 5.3. Alice is on the left and Bob is on the right. They act on their system with their respective measurements represented by $\mathcal{E}$ and $\mathcal{F}$ and after a round of classical communication, they apply the port-processing operations $\mathcal{M}$ and $\mathcal{N}$ respectively.

teleportation here allows to save an exponential amount of entanglement [17] compared to an earlier solution to this problem by Vaidman [31].

6 Port-based teleportation for continuous variables

The main objective of this thesis is to prove that port-based teleportation can also be performed using infinite-dimensional systems. That is, we want to show that it is in principle possible to implement port-based teleportation using quantum optics. This present section is devoted to re-formulating what was stated in the preceding section for continuous variables systems. The results presented in this section constitute our contribution to the understanding of port-based teleportation.

6.1 Figure of merit

Following the same lines as the generalization in the Vaidman-Braunstein-Kimble protocol, the entanglement used will be given by the two-mode squeezed states $|\Phi(r)\rangle$ with parameter r. As we would like our formulation to be compatible with typical applications in quantum optics, we will focus on Gaussian states. More precisely, our task will be to teleport a coherent state $|\alpha\rangle$ taken at random from a Gaussian prior distribution $p_\lambda(\alpha) = \frac{\lambda}{\pi} e^{-\lambda|\alpha|^2}$. This assumption is used for two reasons. The expectation of the energy (i.e. mean photon number) of a coherent state is related to $|\alpha|^2$, so sampling from this distribution implies that we assume states of higher energy are less likely to be picked. This is a fair assumption in general for real life applications. The second reason is a practical one, we will need to compare our results with some kind of measure and prepare protocol to be able to state whether there might be some advantage to use port-based teleportation in this context. As mentioned in section 4.4, Chiribella and Xie [23] found that the optimal fidelity for a measure and prepare protocol in this situation (i.e. given a coherent state with Gaussian prior) is given by $\bar{F} = \frac{\lambda+1}{\lambda+2}$.

As in the finite-dimensional case, we will show that the average fidelity is related to a distinguishability problem (by Theorem 5.1). The following corollary specifies the details of this reformulation.

Corollary 6.1 (Equivalent hypothesis testing problem for coherent states) *Let $|\Phi(r)\rangle_{AB}$ be the two-mode squeezed state of parameter r, let $|\psi_\alpha\rangle = |\alpha\rangle$ be coherent states, and let $p_\alpha = \frac{\lambda}{\pi} e^{-\lambda|\alpha|^2}$ be a centered Gaussian with variance $\frac{1}{2\lambda}$ in $\mathbb{C}$. Then port-based teleportation $\mathcal{T}$ with N ports with resource state $|\Phi(r)\rangle^{\otimes N}$ has average fidelity*

$$\bar{F} = N \frac{\lambda}{\lambda \cosh^2(r) + 1} p_{succ} \tag{41}$$

where p_{succ} is the probability of successfully distinguishing the centered Gaussian states $\rho_i = \tau_{\bar{A}_i}^{\otimes N-1} \otimes$

62

σ_{SA_i}. *Here τ is a thermal state and σ is a mixed state which gives the following covariance matrix for ρ_i*

$$\gamma_{\rho_i} = \bigoplus_{j \neq i}^{N} (\cosh(2r) \mathbb{1}_2)_{A_j} \oplus \left[\mathbb{1}_4 + \frac{2 \cosh^2(r)}{\lambda \cosh^2(r) + 1} \begin{pmatrix} \mathbb{1}_2 & \tanh(r)\sigma_z \\ \tanh(r)\sigma_z & \tanh^2(r)\mathbb{1}_2 \end{pmatrix} \right]_{SA_i}.$$

Proof Our resource state is the two-mode squeezed state $|\Phi(r)\rangle_{A_i B_i} = \frac{1}{\cosh(r)} \sum_{n=0}^{\infty} \tanh^n(r)|n\rangle_{A_i}|n\rangle_{B_i}$ which we know has covariance matrix

$$\gamma = \begin{pmatrix} \cosh(2r)\mathbb{1}_2 & \sinh(2r)\sigma_z \\ \sinh(2r)\sigma_z & \cosh(2r)\mathbb{1}_2 \end{pmatrix}.$$

Tracing out the second mode gives the thermal state with covariance matrix

$$\gamma = \cosh(2r)\mathbb{1}_2$$

and this gives us the covariance matrix of the $N - 1$ modes where we do not have entanglement with

the initial system S. In the formalism of Theorem 5.1, we have to calculate for $|\theta_\alpha\rangle_{SA_i} = |\alpha\rangle_S |\theta_\alpha\rangle_{A_i}$

$$
\begin{aligned}
|\theta_\alpha\rangle_{A_i} &= \frac{1}{\sqrt{q_\alpha}}(\mathbb{1}_{A_i} \otimes \langle\alpha|_{B_i})\frac{1}{\cosh(r)}\sum_{n=0}^{\infty}\tanh^n(r)|n\rangle_{A_i}|n\rangle_{B_i} \\
&= \frac{1}{\sqrt{q_\alpha}}\frac{1}{\cosh(r)}\sum_{n=0}^{\infty}\tanh^n(r)|n\rangle_{A_i}\langle\alpha|n\rangle \\
&= \frac{1}{\sqrt{q_\alpha}}\frac{1}{\cosh(r)}\sum_{n=0}^{\infty}\tanh^n(r)|n\rangle_{A_i}e^{\frac{-|\alpha|^2}{2}}\frac{(\alpha^*)^n}{\sqrt{n!}} \\
&= \frac{e^{\frac{-|\alpha|^2}{2}}}{\cosh(r)}\frac{1}{\sqrt{q_\alpha}}\sum_{n=0}^{\infty}\frac{(\alpha^*\tanh(r))^n}{\sqrt{n!}}|n\rangle_{A_i} \\
&= \frac{1}{\cosh(r)}\frac{1}{\sqrt{q_\alpha}}\exp\left(\frac{(\tanh^2 r - 1)|\alpha|^2}{2}\right)|\tanh(r)\alpha^*\rangle_{A_i} \\
&= \frac{1}{\cosh(r)}\frac{1}{\sqrt{q_\alpha}}\exp\left(\frac{-|\alpha|^2}{2\cosh^2 r}\right)|\tanh(r)\alpha^*\rangle_{A_i}.
\end{aligned}
$$

That allows us to conclude that

$$
q_\alpha = \frac{1}{\cosh^2(r)}\exp\left(-\frac{|\alpha|^2}{\cosh^2 r}\right)
$$

which in turn implies

$$
\int dp(\beta)q_\beta = \frac{\lambda}{\lambda\cosh^2(r) + 1}.
$$

This proves the formula for the fidelity (41). The state of the two entangled systems SA_i has the form

$$
\theta_{SA_i}^\alpha = \int d^2\alpha \frac{\lambda\cosh^2(r) + 1}{\pi\cosh^2(r)}\exp\left(-\frac{\lambda\cosh^2(r) + 1}{\cosh^2(r)}|\alpha|^2\right)|\alpha\rangle\langle\alpha|_S \otimes |\tanh(r)\alpha^*\rangle\langle\tanh(r)\alpha^*|_{A_i}
$$

which has been studied by Namiki [32]. The covariance matrix of such a state is given by

$$\gamma_{\theta_{SA_i}^{\alpha}} = \mathbb{1}_4 + \frac{2\cosh^2(r)}{\lambda\cosh^2(r)+1} \begin{pmatrix} \mathbb{1}_2 & \tanh(r)\sigma_z \\ \tanh(r)\sigma_z & \tanh^2(r)\mathbb{1}_2 \end{pmatrix}.$$

∎

Although the two-mode squeezed state $|\Phi(r)\rangle$ is a perfectly entangled state only in the non-physical limit of infinite squeezing, we have something analogous to the entanglement fidelity for infinite-dimensional systems. It comes up with the teleportation of one mode of a two-mode squeezed state.

Corollary 6.2 (Equivalent hypothesis testing problem for two-mode squeezed states) *The entanglement fidelity for port-based teleportation $\mathcal{T}$ of one mode of a two-mode squeezed state $|\Phi(r_1)\rangle$ with parameter r_1 and N copies of $|\Phi(r_2)\rangle$ as a resource state is given by*

$$F_{ent}(\mathcal{T},|\Phi(r_1)\rangle) = \frac{N}{\cosh^4(r_1)\cosh^2(r_2) - \sinh^4(r_1)\sinh^2(r_2)}p_{succ}$$

where p_{succ} is the probability of distinguishing the states

$$\rho_i = \tilde{\Phi}_{SA_i} \otimes \tau_{\bar{A}_i}^{\otimes(N-1)}.$$

Here $|\tilde{\Phi}(r')\rangle_{SA_i}$ is a two-mode squeezed state with parameter $r' = \tanh^{-1}(\tanh^2(r_1)\tanh(r_2))$ and τ is a thermal state of parameter r_2.

Proof We use the results from Theorem 5.1 to prove our claim. The calculation for θ_{SA_i} (37) reads

$$
\begin{aligned}
|\theta\rangle_{SA_i} &= \frac{1}{\sqrt{q}}(\mathbb{1}_{SA_i} \otimes \langle\Phi(r_1)|_{DB_i})|\Phi(r_1)\rangle_{DS}|\Phi(r_2)\rangle_{A_iB_i} \\
&= \frac{1}{\cosh^2(r_1)\cosh(r_2)\sqrt{q}} \sum_n (\tanh^2(r_1)\tanh(r_2))^n|nn\rangle_{SA_i} \\
&= \frac{1}{\cosh^2(r_1)\cosh(r_2)\sqrt{1-\tanh^4(r_1)\tanh^2(r_2)}\sqrt{q}}|\tilde{\Phi}\rangle_{SA_i} \\
&= \frac{1}{\sqrt{\cosh^4(r_1)\cosh^2(r_2)-\sinh^4(r_1)\sinh^2(r_2)}\sqrt{q}}|\tilde{\Phi}\rangle_{SA_i}.
\end{aligned}
$$

From these calculations, we see that $q = \frac{1}{\cosh^4(r_1)\cosh^2(r_2)-\sinh^4(r_1)\sinh^2(r_2)}$ and $\tanh(r') = \tanh^2(r_1)\tanh(r_2)$ and the claim follows. ∎

We can see that the interpretation of the entanglement fidelity in this case relates directly to what we had for the finite-dimensional case. We previously had maximally mixed states on $N-1$ ports where we now have thermal states with parameter r_2 on $N-1$ ports. In both cases, the system S is entangled with another of the N ports, in the finite-dimensional case this was given by a Bell state and for the infinite-dimensional case it is described by the squeezing parameter of a two-mode squeezed state.

6.2 Entanglement fidelity vs average fidelity for continuous variables

It has already been mentioned that there is a relation between the average fidelity and the entanglement fidelity for finite-dimensional systems, see equation (38). Let us discuss the existence of this kind of relationship for infinite-dimensional systems. Intuitively, we expect a link between the fidelity when teleporting a two-mode squeezed state and the average fidelity for the teleportation of a coherent state with Gaussian prior. Indeed, doing heterodyne measurement (measuring in the basis $\{|\alpha\rangle\}_\alpha$) on one mode of a two-mode squeezed state $|\Phi(r)\rangle$ will result in the state (see

Lemma 3.3)

$$|\alpha^* \tanh(r)\rangle \qquad \text{with probability} \qquad p(\alpha) = \frac{1}{\pi \cosh^2(r)} \exp\left(\frac{-|\alpha|^2}{\cosh^2(r)}\right) \qquad (42)$$

on the unmeasured mode and produce the classical output α.

The two cases are not strictly equivalent however. Because the heterodyne measurement is done on one mode only, it cannot have an observable influence on the mode to be teleported. If we do not have knowledge of the outcome, the state to be teleported would be described as a mixture of coherent states with Gaussian prior. This is how we defined thermal states in Section 3.2.3, which are different from coherent states. Therefore, we cannot just replace $\lambda = \frac{1}{\sinh^2(r)}$ in Lemma 6.1 and use the same analysis. We want to establish a relation between the fidelities with and without the measurement done on a two-mode squeezed state. It will be useful to first consider the following slightly more general situation.

Lemma 6.3 (Relation between average and entanglement fidelity) *Suppose system D of a bipartite state $|\Phi\rangle_{DS}$ is measured using a measurement $\mathcal{M} = \{E_i\}_i$, resulting in a classical output i with probability $p(i)$ and a post-measurement state $|\phi_i\rangle$ on the unmeasured system S. Then*

$$F_{ent}(\mathcal{T}, |\Phi\rangle) \leq \bar{F}(\mathcal{T}) \qquad (43)$$

for any teleportation map $\mathcal{T}$ applied to system S. Here the average is taken over the ensemble $\{p_i, |\phi_i\rangle\}$.

Proof The resulting state when measuring D is

$$(\mathcal{M} \otimes I)(|\Phi\rangle\langle\Phi|) = \sum_i p(i)|i\rangle\langle i| \otimes |\phi_i\rangle\langle\phi_i|_S \ ,$$

where i denotes the value of a classical register $|i\rangle\langle i|$ that allows us to keep track of the measurement outcome. Since it is a classical register, the states $\{|i\rangle\}_i$ are orthogonal, $\langle i|j\rangle = \delta_{ij}$. To prove (43), we use that the fidelity is monotonic under quantum operations (we cannot increase the distinguishability of two states by application of a CPTP map $\mathcal{M}$)

$$F(\rho, \sigma) \leq F(\mathcal{M}(\rho), \mathcal{M}(\sigma)).$$

This implies that

$$F_{ent}(\mathcal{T}, |\Phi\rangle) = F(\Phi, (I \otimes \mathcal{T})(\Phi)) \leq F((\mathcal{M} \otimes I)(\Phi), (\mathcal{M} \otimes \mathcal{T})(\Phi)) \tag{44}$$

where $\Phi = |\Phi\rangle\langle\Phi|$ for simplicity. We will show that

$$F((\mathcal{M} \otimes I)(\Phi), (\mathcal{M} \otimes \mathcal{T})(\Phi)) \leq \bar{F}(\mathcal{T}). \tag{45}$$

To do so, we directly compute

$$F((\mathcal{M} \otimes I)(\Phi), (\mathcal{M} \otimes \mathcal{T})(\Phi)) = F\left(\sum_i p(i)|i\rangle\langle i| \otimes |\phi_i\rangle\langle\phi_i|, \sum_j p(j)|j\rangle\langle j| \otimes \mathcal{T}(|\phi_j\rangle\langle\phi_j|)\right). \tag{46}$$

Now recall that

$$\sqrt{F(\rho, \sigma)} = \text{tr}\left(\sqrt{\sqrt{\sigma}\rho\sqrt{\sigma}}\right)$$

and because the states of the classical register are orthogonal we also have

$$\sqrt{\sum_i p(i)|i\rangle\langle i| \otimes \rho_i} = \sum_i \sqrt{p(i)}|i\rangle\langle i| \otimes \sqrt{\rho_i}.$$

68

Inserting this into (46) gives (with $\sqrt{\sigma} = \sum_i \sqrt{p(i)}|i\rangle\langle i|\otimes|\phi_i\rangle\langle\phi_i|$ and $\rho = \sum_j p(j)|j\rangle\langle j|\otimes\mathcal{T}(|\phi_j\rangle\langle\phi_j|)$

$$
\begin{aligned}
\sqrt{F((\mathcal{M}\otimes I)(\Phi), (\mathcal{M}\otimes\mathcal{E})(\Phi))} &= \mathsf{tr}\left(\sqrt{\sum_i p^2(i)|i\rangle\langle i|\otimes|\phi_i\rangle\langle\phi_i|\mathcal{T}(\phi_i)|\phi_i\rangle\langle\phi_i|}\right)\\
&= \sum_i p(i)\sqrt{\langle\phi_i|\mathcal{T}(\phi_i)|\phi_i\rangle}\\
&\leq \sqrt{\sum_i p(i)\langle\phi_i|\mathcal{T}(\phi_i)|\phi_i\rangle}\\
&= \sqrt{\bar{F}(\mathcal{T})}\;,
\end{aligned}
$$

where we used concavity of the square root. We obtain (45), which together with (44) implies the claim (43). ∎

In other words, this shows that $F_{ent} \leq \bar{F}$ so the entanglement fidelity is always smaller than the corresponding average fidelity. We are now ready to prove the main statement of this section.

Theorem 6.4 (Average and entanglement fidelity for two-mode squeezed states) *The fidelity $F_{ent}(\mathcal{T}, |\Phi(r)\rangle)$ of teleporting one mode of a two-mode squeezed state $|\Phi(r)\rangle$ of parameter r is related to the average fidelity $\bar{F}(\mathcal{T})$ of teleporting a coherent state $|\alpha\rangle$ with prior probability $p(\alpha) = \frac{1}{\pi\sinh^2(r)}\exp\left(\frac{-|\alpha|^2}{\sinh^2(r)}\right)$ by the relation*

$$
F_{ent}(\mathcal{T}, |\Phi(r)\rangle) \leq \bar{F}(\mathcal{T}).
$$

Proof We apply Lemma 6.3 to the two-mode squeezed state $|\Phi(r)\rangle_{DS}$ with the heterodyne measurement $\mathcal{M}$ applied to D. As mentioned above (Eq. (42)), this yields the state $|\beta^*\tanh(r)\rangle$ on S with probability $\tilde{p}(\beta) = \frac{1}{\pi\cosh^2(r)}\exp(-\frac{|\beta|^2}{\cosh^2(r)})$. We make the variable substitution $\alpha = \beta^*\tanh(r)$.

69

We then get the coherent state $|\alpha\rangle$ with probability

$$p(\alpha) = \frac{1}{\tanh^2(r)} \tilde{p}\left(\frac{\alpha^*}{\tanh(r)}\right) = \frac{1}{\pi \sinh^2(r)} \exp\left(-\frac{|\alpha|^2}{\sinh^2(r)}\right)$$

where the factor $\frac{1}{\tanh^2(r)}$ is the Jacobian associated with the variable substitution. The claim therefore follows from Lemma 6.3. ∎

In conclusion, if we are able to teleport a two-mode squeezed state, then we also have the capacity to teleport a coherent state taken at random from a Gaussian distribution.

6.3 Protocol for teleporting coherent states with squeezed state resources

In this section, we will demonstrate the possibility of teleporting coherent states given a suitable set of restrictions on the resources we can use. The protocol has two main parts. The first one concentrates entanglement from our resources into finite-dimensional entangled pairs. The second one gives an approximation of a coherent state by a finite-dimensional system. Combining these two components, we can use known results about port-based teleportation for finite-dimensional systems.

This proves that port-based teleportation for continuous variable can be reduced to the teleportation of finite-dimensional systems. Unfortunately, the resulting protocol does not directly work on infinite-dimensional systems as the Vaidman-Braustein-Kimble protocol does for standard teleportation. In particular, our existence proof does not provide a way to implement port-based teleportation using standard quantum optics elements.

Our protocol relies on a form of non-interactive entanglement concentration. There is one significant difference to the usual port-based teleportation scheme: it requires pre- and post-processing involving quantum operations also on Bob's side. As a consequence, Bob needs to be able to accomplish more than just discarding quantum systems.

6.3.1 Non-interactive entanglement concentration

In this section, we show how to extract maximally entangled states from non-maximally entangled bipartite resources without using classical communication. Assume we have n copies of a bipartite entangled state $|\phi\rangle = \sum_{j=1}^{D} \sqrt{p_j}|e_j\rangle|f_j\rangle \in \mathbb{C}^D \otimes \mathbb{C}^D$ where $p_\phi = (p_1, \ldots, p_D)$ is the Schmidt spectrum and $\{|e_j\rangle\}_j$ and $\{|f_j\rangle\}_j$ are the orthonormal Schmidt bases. Our goal is to extract N maximally entangled states $|\Phi_d^+\rangle = \frac{1}{\sqrt{d}} \sum_{j=1}^{d} |j\rangle|j\rangle$ from $|\phi\rangle^{\otimes n}$. We show that the number N that can be extracted is related to the entropy $H(p_\phi) = -\sum_{j=1}^{D} p_j \log_2 p_j$ of the distribution p_ϕ.

A procedure to accomplish this task was developed by Hayashi and Matsumoto [22]. Remarkably, it is universal in the sense that it requires no knowledge of the Schmidt bases. They exploited the symmetries of a system consisting of multiple copies of an unknown pure state. The first observation here is that the input is independent on the reordering of the copies i.e. $|\phi\rangle^{\otimes n}$ is invariant under the action of the permutation group S_n. A second observation is that the application of local unitaries $(U \otimes V)^{\otimes n}$ with U and V being elements of $SU(D)$ cannot affect the entanglement of $|\phi\rangle^{\otimes n}$. Indeed, this corresponds to a change in the Schmidt bases. Now, the group of permutations S_n acts on the n factors on Alice's side, and commutes with the action $U^{\otimes n}$ of $SU(D)$. In other words, Alice's Hilbert space decomposes as

$$\mathcal{H}_A^{\otimes n} = \bigoplus_{\lambda:\lambda \vdash n} \mathcal{U}_{\lambda A} \otimes \mathcal{V}_{\lambda A}$$

where the sum is over partitions λ of n, and where $\mathcal{U}_{\lambda A}$ and $\mathcal{V}_{\lambda A}$ are irreducible representations of $SU(D)$ and S_n, respectively. This result is known as Schur-Weyl duality. An analogous decomposition can be given for Bob's Hilbert space $\mathcal{H}_B^{\otimes n}$. By the mentioned invariance of $|\phi\rangle^{\otimes n}$, it must have the form

$$|\phi\rangle^{\otimes n} = \bigoplus_{\lambda:\lambda \vdash n} a_\lambda |\phi_\lambda\rangle|\Phi_\lambda\rangle \qquad \text{where} \qquad |\phi_\lambda\rangle \in \mathcal{U}_{\lambda A} \otimes \mathcal{U}_{\lambda B}, |\Phi_\lambda\rangle \in \mathcal{V}_{\lambda A} \otimes \mathcal{V}_{\lambda B}.$$

In this decomposition, a_λ and $|\phi_\lambda\rangle$ both depend on the particular form of $|\phi\rangle$ (i.e., the Schmidt bases and spectrum), but more importantly, $|\Phi_\lambda\rangle$ is a maximally entangled state of dimension $\dim \mathcal{V}_\lambda$ independent of $|\phi\rangle$. This means that even without knowing the specific form of $|\phi\rangle$, there are maximally entangled states accessible to two people sharing the bipartite state $|\phi\rangle^{\otimes n}$. They simply need to apply their respective projective measurement onto the subspaces $\{\mathcal{U}_{\lambda x} \otimes \mathcal{V}_{\lambda x}\}_\lambda$ $(x = A, B)$ to have their state collapse to

$$|\phi_\lambda\rangle|\Phi_\lambda\rangle \in (\mathcal{U}_{\lambda A} \otimes \mathcal{U}_{\lambda B}) \otimes (\mathcal{V}_{\lambda A} \otimes \mathcal{V}_{\lambda B})$$

and then tracing out the first part on $\mathcal{U}_{\lambda x}$, $x = A, B$ leaves them with a maximally entangled state. The measurement done by either Alice or Bob will project the system onto a specific subspace identified by λ. The measurement of the other individual will return the same index so no classical communication is required. For instance, in the qubit case it would be the measurement of the total spin of the system in the z direction. The probabilities of the measurement to return a given dimension $\dim \mathcal{V}_\lambda$ for the entanglement depend on the coefficients $\{a_\lambda\}_\lambda$. To obtain entanglement of a specific dimension d, we perform an additional projection.

The following (probabilistic) procedure explains in more detail how this measurement is done with the decomposition introduced above. It is a useful building block for port-based teleportation starting from non-maximal entanglement. This protocol depends on some rate parameter R.

Protocol 6.1: Non-interactive entanglement concentration

Input: $|\phi\rangle^{\otimes n}$, where $|\phi\rangle$ has Schmidt spectrum p_ϕ, and a chosen value of the parameter R respecting $R < H(p_\phi)$. Output: success/fail. If the protocol succeeds, the output is $m \in \mathbb{N}$ and $|\Phi_d^+\rangle^{\otimes m}$.

1. Alice and Bob apply their projective measurement $\{\mathcal{U}_{\lambda x} \otimes \mathcal{V}_{\lambda x}\}_\lambda$ $(x = A, B)$ on their respective systems. They obtain the classical outcome λ. If λ is such that the dimension of the corresponding space $\dim(\mathcal{V}_\lambda)$ is smaller than 2^{nR}, they abort the protocol. Otherwise, Alice and Bob trace out the system $\mathcal{U}_{\lambda x}$ $(x = A, B)$ and then share the maximally entangled state $|\Phi_\lambda\rangle$ of dimension $\dim \mathcal{V}_\lambda$.

2. Define $m := \lfloor \log_d \dim \mathcal{V}_\lambda \rfloor$. Alice and Bob do a projection onto the subspace spanned by the first m basis elements of the Schmidt basis of the maximally entangled state $|\Phi_\lambda\rangle$. Since the state $|\Phi_\lambda\rangle$ is maximally entangled, they obtain m copies of the maximally entangled state $|\Phi_d^+\rangle$ if the projection succeeds. If the projection fails, Alice and Bob abort the protocol.

Note that the last step in this protocol also does not require any communication since Alice and Bob's outcome will be identical. The success probability of this protocol and the resource requirements are given by the following theorem.

Theorem 6.5 (Universal non-interactive entanglement concentration) *Consider Protocol 6.1, which takes as input n copies of a bipartite state $|\phi\rangle \in \mathbb{C}^D \otimes \mathbb{C}^D$ with Schmidt spectrum p_ϕ. For any $R < H(p_\phi)$, it outputs at least $\lfloor nR \log_d 2 \rfloor$ copies of the maximally entangled state $|\Phi_d^+\rangle$ if the protocol succeeds. This happens with probability at least $\frac{1-\nu(n)}{d}$ where $\nu(n)$ is exponentially small in n for n large enough.*

Proof We have two potential sources of failure in this protocol.
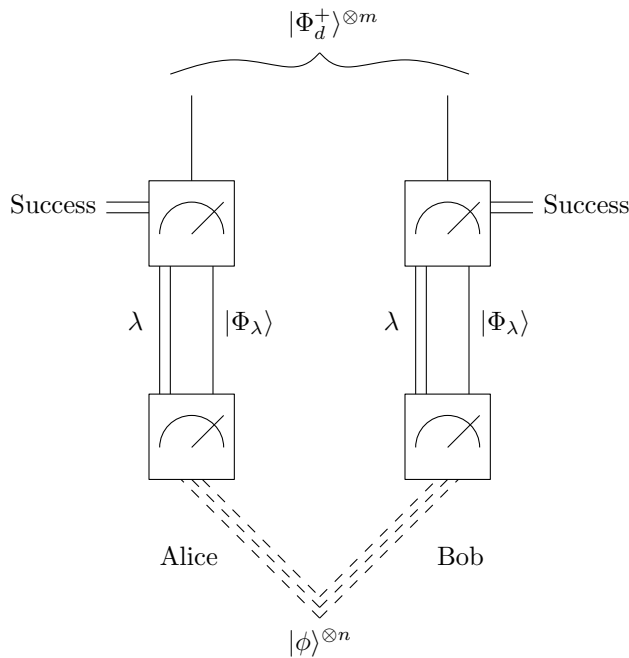
Figure 8: This represents the non-interactive entanglement concentration Protocol 6.1.

1. The projection $\{\mathcal{U}_{\lambda x} \otimes \mathcal{V}_{\lambda x}\}_\lambda$ (where $x = A$ or $x = B$) could return a partition λ for which $\dim \mathcal{V}_\lambda < 2^{nR}$ in which case we cannot extract enough maximally entangled states.

2. The projection onto the first $\lfloor \log_d \mathcal{V}_\lambda \rfloor$ orthonormal basis states of the maximally entangled state $|\Phi_\lambda\rangle \in \mathcal{V}_{\lambda A} \otimes \mathcal{V}_{\lambda B}$ might fail.

The first source of failure has already been studied by Matsumoto and Hayashi [21]: We have to analyze the probability that the projection $\{\mathcal{U}_\lambda \otimes \mathcal{V}_\lambda\}_\lambda$ returns a partition λ for which $\dim \mathcal{V}_\lambda < 2^{nR}$. Matsumoto and Hayashi showed that the probability that the dimension $\dim \mathcal{V}_\lambda$ is less than roughly $2^{nH(p_\phi)}$ decreases exponentially in n. More specifically, they showed that (see Equation (5) in [21])

$$\lim_{n \to \infty} -\frac{1}{n} \log \sum_{\lambda : \dim \mathcal{V}_\lambda \leq 2^{nR}} a_\lambda^2 = D(R \| p_\phi) \tag{47}$$

where

$$D(R\|p_\phi) = \begin{cases} \min_{q:H(q)\geq R} D(q\|p) & \text{if } H(p_\phi) \leq R \\ \min_{q:H(q)\leq R} D(q\|p) & \text{if } H(p_\phi) > R \end{cases}.$$

Identity (47) tells us that for any $\epsilon > 0$, there exists $n_0 = n_0(\epsilon)$ such that

$$\sum_{\lambda:\dim \mathcal{V}_\lambda \leq 2^{nR}} a_\lambda^2 \leq 2^{-n(D(R\|p_\phi)-\epsilon)} \qquad \text{for all } n \geq n_0(\epsilon).$$

Since the quantity $D(R\|p_\phi)$ is positive for any $R < H(p_\phi)$, we conclude that (for any $0 < \epsilon < D(R\|p_\phi)$ and $n \geq n_0(\epsilon)$) the probability of getting a λ with $\dim \mathcal{V}_\lambda < 2^{nR}$ is exponentially close to 0 in n. Note that this corresponds to getting fewer than $\lfloor \log_d \dim V_\lambda \rfloor \leq \lfloor \log_d 2^{nR} \rfloor = \lfloor nR \log_d 2 \rfloor$ copies of the maximally entangled state $|\Phi_d^+\rangle$. (In fact, there is an equation analogous to (47) in the other direction. It implies that the probability of getting more than $nR \log_d 2$ copies of $|\Phi_d^+\rangle$ is exponentially close to 0 in n as well. However, we do not need this statement here.) Therefore we will say that this projection succeeds with probability $p_1 = 1 - \nu(n)$ where $\nu(n)$ goes to 0 exponentially fast.

Now suppose that $\dim \mathcal{V}_\lambda \geq 2^{nR}$ such that $\lfloor \log_d \dim \mathcal{V}_\lambda \rfloor \geq \lfloor \log_d 2^{nR} \rfloor = \lfloor nR \log_d 2 \rfloor$ and let $m := \lfloor \log_d \dim \mathcal{V}_\lambda \rfloor$. By definition of m, we have

$$d^m \leq \dim \mathcal{V}_\lambda \leq d^{m+1} - 1. \tag{48}$$

Projecting the state $|\Phi_\lambda\rangle$ (which has uniform Schmidt spectrum) onto the d^m-dimensional subspace associated with the first d^m basis elements succeeds with probability $p_2 = d^m/\dim \mathcal{V}_\lambda$, which is bounded by $p_2 \geq d^m/(d^{m+1} - 1) \geq 1/d$ by (48).

The overall probability of success for the protocol is then given by the probability the first porjection succeeds multiplied by the probability the second projection succeeds conditioned on the

first one also being successful. This is given by the multiplication of p_1 and p_2. This concludes the proof. ∎

Theorem 6.5 tells us that the output and success probability of this protocol only depend on the entropy of the resource state $|\phi\rangle$, in particular it is independent of the dimension D. This is logical because we could embed any state $|\phi\rangle$ into a bigger space of dimension $D' > D$ (which would only add 0's to the Schmidt spectrum) and this should not change the entanglement. We can therefore apply the result to two-mode squeezed states $|\Phi(r)\rangle$. This state has Schmidt spectrum $p_n = (\tanh^{2n}(r))/\cosh(r)^2 = (1 - \xi^2)\xi^{2n}$, $n = 0, 1, \ldots$, where $\xi = \tanh(r)$ as can be seen from (32). Its entropy is

$$
\begin{aligned}
H(p_{|\Phi(r)\rangle}) &= -\sum_n (1 - \xi^2)\xi^{2n} \log((1 - \xi^2)\xi^{2n}) \\
&= -(1 - \xi^2)\log(1 - \xi^2)\sum_n \xi^{2n} - (1 - \xi^2)\sum_n \xi^{2n}\log(\xi^{2n}) \\
&= -\log(1 - \xi^2) - (1 - \xi^2)(\log\xi)\sum_n \xi^{2n}(2n) \\
&= -\log(1 - \xi^2) - (1 - \xi^2)(\log\xi)\frac{2\xi^2}{(1 - \xi^2)^2} \\
&= -\log(1 - \xi^2) - 2(\log\xi)\cdot\frac{\xi^2}{1 - \xi^2} \\
&= 2\log(\cosh(r)) - 2\sinh(r)\log(\tanh(r)).
\end{aligned}
\tag{49}
$$

Based on Protocol 6.1, it is straightforward to give a protocol for teleporting qudits using non-maximally entangled states. The resulting protocol takes the following form.

> **Protocol 6.2: Port-based qudit teleportation with non-maximally entangled resource $|\phi\rangle^{\otimes n}$**
>
> Input: resource $|\phi\rangle^{\otimes n}$ and state $|\Psi\rangle$ to be teleported. Output: success/fail and if the protocol succeeds, a state $|\Psi'\rangle$ on Bob's side that approximates $|\Psi\rangle$.
>
> **1:** Alice and Bob run the Protocol 6.1 on their input $|\phi\rangle^{\otimes n}$ for some suitably chosen $R < H(p_\phi)$. If sucessful, they obtain $N = \lfloor nR \log_d 2 \rfloor$ maximally entangled states $|\Phi_d^+\rangle$.
>
> **2:** Alice and Bob then run the port-based teleportation protocol 5.1 for qudits using the resource $|\Phi_d^+\rangle^{\otimes N}$ and the state $|\Psi\rangle$. After Bob has received Alice's classical information and discarded the appropriate ports, he has the state $|\Psi'\rangle$.

A key property of this protocol is that the state to be teleported is untouched in case the entanglement concentration protocol is unsuccessful. This means that Alice and Bob can repeat (assuming they have enough entanglement) the first step of Protocol 6.2 until they have enough maximal entanglement for the second step. Assuming we want to perform port-based teleportation using entanglement concentration only once with given entanglement fidelity, how many copies of $|\phi\rangle$ do we need? We address this question in the following corollary.

Corollary 6.6 (Teleportation for non-maximal entanglement) *Let $\epsilon > 0$, $\delta > 0$ and $R < H(p_\phi)$. We need $n \geq \frac{2d^2}{\epsilon R \log_d 2}$ for the entanglement fidelity of the teleportation process $\mathcal{T}$ to satisfy $F_{ent}(\mathcal{T}) \geq 1 - \epsilon$ when Protocol 6.2 succeeds. Similarly, we need $n \geq \frac{32 \cdot d^4}{\delta^2 R \log_d 2}$ for the teleportation process $\mathcal{T}$ to be whithin distance δ of the identity channel, $\|\mathcal{T} - \mathbb{I}\|_\diamond \leq \delta$, when successfully using Protocol 6.2. The protocol is successful with probability at least $\frac{1 - \nu(n)}{d}$ (where $\nu(n)$ is exponentially small in n).*

Proof The subprotocol 6.1, if successful, generates $N = \lfloor nR \log_d 2 \rfloor$ copies of the maximally entangled state $|\Phi_d^+\rangle$. Using this for port-based teleportation gives, according to (39), an entanglement

fidelity of

$$F_{ent}(\mathcal{T}) \geq 1 - \frac{d^2}{N} \geq 1 - \frac{d^2}{nR \log_d 2 - 1} \geq 1 - \frac{2d^2}{nR \log_d 2}$$

where we used $\lfloor x \rfloor \geq x - 1$ and $\frac{1}{y-1} \leq \frac{2}{y}$ for $y > 2$ For this to be lower bounded by $1 - \epsilon$, we need $1 - \frac{2d^2}{nR \log_d 2} \geq 1 - \epsilon$ or $n \geq \frac{2d^2}{\epsilon R \log_d 2}$, which is our assumption.

The statement for the diamond norm follows in a similar way from (40) for d-dimensional port-based teleportation since

$$\|\mathcal{T} - \mathbb{I}\|_\diamond \leq \frac{4d^2}{\sqrt{N}} \leq \frac{4d^2}{\sqrt{nR \log_d 2 - 1}} \leq \frac{\sqrt{2} \cdot 4d^2}{\sqrt{nR \log_d 2}} \ ,$$

and the latter expression is smaller than δ if $n \geq \frac{32 \cdot d^4}{\delta^2 R \log_d 2}$. ∎

In particular, when teleporting m qubits ($d = 2^m$) using copies of a two-qubit entangled state $|\phi\rangle \in \mathbb{C}^2 \otimes \mathbb{C}^2$, this means we need at least $n \geq (m \cdot 2^{2m+1})/(\epsilon H(p_\phi))$ copies of $|\phi\rangle$ (i.e., an exponential number in m), and the teleportation succeeds with probability approximately $\frac{1}{2}$.

6.3.2 Converting coherent states to qubits

Corollary 6.6 allows us to use non-maximally entangled resource states such as the two-mode squeezed state, but the input state needs to be a finite-dimensional system. More specifically, to teleport coherent states, we need a procedure for converting coherent states to qubits. Of course, this procedure will only provide an approximation of the coherent state. One possibility is to use a number state projection, but this may not be feasible. A simpler procedure involves a beam-splitter-network (i.e., unitary U) as shown in Fig. 9. It consists of an encoding map $\mathcal{E}_M$ and a decoding map $\mathcal{D}_M$ which are applied on Alice and Bob's sides, respectively, that are parametrized by some number M determining the quality of the conversion. A similar procedure is used for example in [33].

The idea is to distribute the coherent state to many systems. Doing so, we expect its energy to be divided between the different systems. For M large enough, each system should have 0 or 1 photon with high probability. At this point, we can do a projection on each system to obtain a qubit and this measurement should not perturb the systems too much. More explicitely, the encoding is described by the following protocol (see also Figure 9).

Protocol 6.3: Encoding $\mathcal{E}_M$

Input: $|\alpha\rangle$ (unknown) coherent state. Output: success/fail. If the protocol succeeds, the output is the M-qubit state $|\phi_{\alpha,M}\rangle = \left(\frac{1}{\sqrt{1+|\alpha|^2/M}} \left(|0\rangle + \frac{\alpha}{\sqrt{M}}|1\rangle \right) \right)^{\otimes M}$.

1. Alice combines the input state $|\alpha\rangle$ with $M-1$ vacuum states using the multi-mode beam splitter U, getting the state $|\frac{\alpha}{\sqrt{M}}\rangle^{\otimes M}$.

2. Alice subsequently performs a projective measurement $\{\Pi = |0\rangle\langle 0| + |1\rangle\langle 1|, \mathbb{1} - \Pi\}$ to each of these M modes. The protocol is successful if each measurement gives outcome Π. In this case, the output state is the post-measurement state (after projection).

The point of this procedure is that the output $|\phi_{\alpha,M}\rangle \in (\mathbb{C}^2)^{\otimes M}$ is a state of M qubits; nevertheless, it approximates the state $|\frac{\alpha}{\sqrt{M}}\rangle^{\otimes M}$. In particular, if Alice can teleport this M-qubit state to Bob, then Bob can recover an approximation to $|\alpha\rangle$ by applying the following decoding procedure (see Figure 9).

Protocol 6.4: Decoding $\mathcal{D}_M$

Input: M-qubit state ρ. Output: 1-mode state.

1. Bob applies $U^\dagger$, where U is the multi-mode beam splitter.

2. Bob traces out all but the first mode.

The following lemma describes the effect of this encoding and decoding procedure.
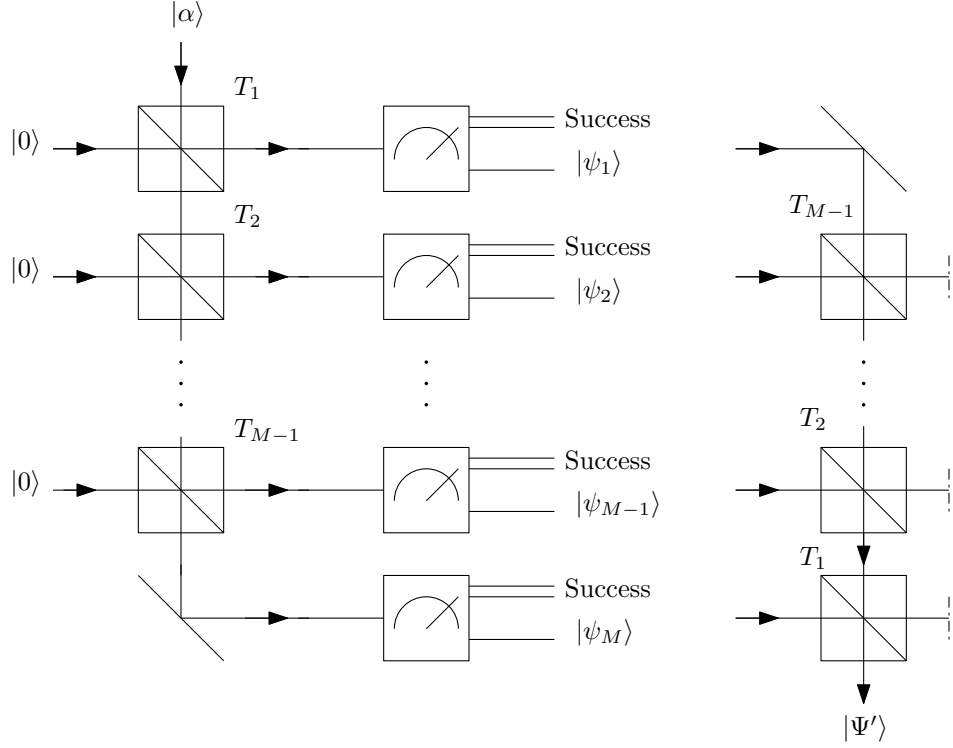
Figure 9: On the left is the beam-splitter-network for Protocol 6.3. The input state is given by $|\alpha\rangle|0\rangle^{\otimes M-1}$. There are M beam-splitter with transmittivity $T_n = \frac{1}{M-(n-1)}$ and one mirror. The intermediate global state is $|\frac{\alpha}{\sqrt{M}}\rangle^{\otimes M}$. Each projection measurement will return classical information (success or failure) and a quantum state $|\psi\rangle = \frac{1}{\sqrt{1+|\alpha|^2/M}}\left(|0\rangle + \frac{\alpha}{\sqrt{M}}|1\rangle\right)$ in the case of success. On the right is the beam-splitter-network for Protocol 6.4, which is essentially the reversed image of the encoding. The output is noted $|\Psi'\rangle$ and the other systems are discarded.

Lemma 6.7 (Behaviour of encoding/decoding) *Consider the encoding process $\mathcal{E}_M$ described by Protocol 6.3 (also see Fig. 9). The probability that the procedure succeeds is $p_\alpha(M) = e^{-|\alpha|^2}(1 + \frac{|\alpha|^2}{M})^M$. In particular, $p_\alpha(M) \to 1$ for $M \to \infty$. In that case, we also have by considering the decoding procedure $\mathcal{D}_M$ from Protocol 6.4*

$$\left\| |\alpha\rangle\langle\alpha| - \mathcal{D}_M(\mathcal{E}_M(|\alpha\rangle\langle\alpha|)) \right\|_1 \leq \sqrt{1 - p_\alpha(M)}. \tag{50}$$

Proof In Step 1, the input state $|\alpha\rangle$ gets converted into the state $|\alpha/\sqrt{M}\rangle^{\otimes M} = U(|\alpha\rangle \otimes |0\rangle^{\otimes M-1})$. In Step 2, each mode in this product is projected onto the span of $|0\rangle$ and $|1\rangle$.

The probability of successfully projecting the coherent states of each system onto the span of $|0\rangle$ and $|1\rangle$ is given by (see (15))

$$p_\alpha(M) = \left(e^{-|\alpha|^2/M}(1 + \frac{|\alpha|^2}{M}) \right)^M$$

which is the first claim. Because $|\phi_{\alpha,M}\rangle = \frac{1}{\sqrt{p_\alpha(M)}}(\otimes_j \Pi_j)|\frac{\alpha}{\sqrt{M}}\rangle^{\otimes M}$, we also have

$$F(\langle\frac{\alpha}{\sqrt{M}}|^{\otimes M}, |\phi_{\alpha,M}\rangle) = \left| \langle\frac{\alpha}{\sqrt{M}}|^{\otimes M}|\phi_{\alpha,M}\rangle \right|^2 = p_\alpha(M).$$

Then from (5) it follows that

$$\left\| |\frac{\alpha}{\sqrt{M}}\rangle\langle\frac{\alpha}{\sqrt{M}}|^{\otimes M} - |\phi_{\alpha,M}\rangle\langle\phi_{\alpha,M}| \right\|_1 \leq \sqrt{1 - p_\alpha(M)}.. \tag{51}$$

Finally, (50) follows because the trace distance is monotonic under applying the decoding map $\mathcal{D}_M$.

∎

The expression for $p_\alpha(M)$ shows that the encoding works better if the original state $|\alpha\rangle$ has small mean photon number $|\alpha|^2$. This is consistent with our interpretation, less energy to distribute

between the systems means that it is easier to get only 0 or 1 photon in each system. Eq. (50) shows that Bob can recover the state $|\alpha\rangle$ up to a small error (if M is large enough).

Modified protocol for port-based teleportation

Combining the protocols for encoding, teleporting a state with non-maximal entanglement and decoding, we obtain a modified version of port-based teleportation. It accomplishes our initial goal which was to teleport coherent states using two-mode squeezed states (see also Figure 10). This is our main result.

Protocol 6.5: Port-based continuous-variable teleportation with squeezed state resource

Input: $|\phi(r)\rangle^{\otimes n}$, where $|\phi(r)\rangle$ is the two-mode squeezed state, and one-mode state $|\Psi\rangle$ to be teleported. Output: success/fail. If the protocol succeeds, a state $|\Psi'\rangle$ at Bob's side that approximates $|\Psi\rangle$.

1. For some appropriately chosen M, Alice applies the encoding map $\mathcal{E}_M$ to $|\Psi\rangle$.

2. If it succeeds, Alice and Bob run Protocol 6.2 using their resource state $|\phi(r)\rangle^{\otimes n}$ and the input $\mathcal{E}_M(|\Psi\rangle\langle\Psi|)$. This subprotocol outputs a quantum state at Bob's site.

3. If it succeeds, Bob applies the decoding map $\mathcal{D}_M$ to obtain $|\Psi'\rangle$.

We presented this protocol with the idea that Alice and Bob wanted to transmit the quantum state $|\Psi\rangle$ directly. Of course, if one is concerned with the applications of port-based teleportation, we need to modify the protocol a little bit. The applications require Bob to act on the output state before having the classical information from Alice that allows him to identify on which port $|\Psi'\rangle$ is. In this case, Bob applies the decoding scheme on every port he has and does not discard them. He can follow any procedure the application requires him to do. The output of this modified version of the protocol would be an N-mode continuous-variable state with a classical index $j \in \{1, \ldots, N\}$.
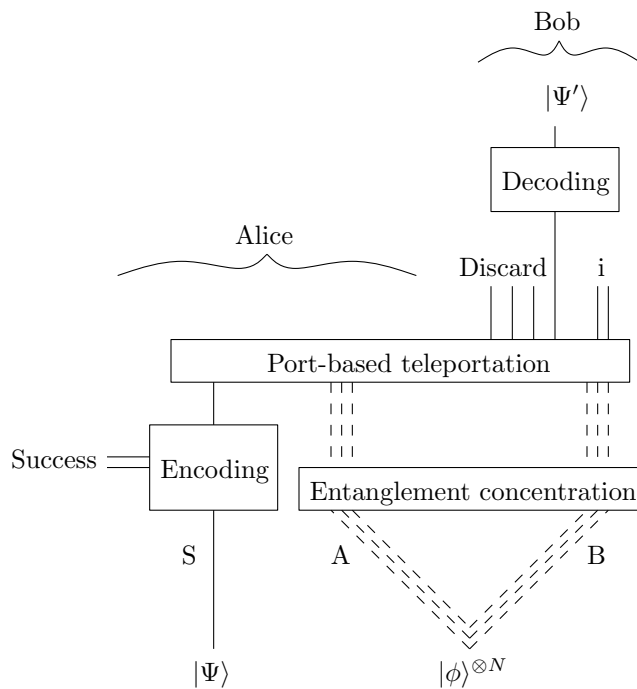
Figure 10: Representation of the Protocol 6.5. The entanglement concentration and port-based teleportation are used as black boxes here, but we still show explicitely the discarding operation done by Bob with the classical information he received. The pre-processing is represented by the measurement on the input and the entanglement concentration of the resource states.

Again, we study how much entanglement is required to obtain an output state close to the input state when we perform this modified version of port-based teleportation. We present our results in this theorem.

Theorem 6.8 (Port-based teleportation for continuous variables) *Let $\epsilon > 0$ and $R < H(p_{|\Phi(r)\rangle})$ (cf. (49)). The Protocol 6.5 used to teleport a coherent state $|\alpha\rangle$ using n copies of a two-mode squeezed state $|\Phi(r)\rangle$ succeeds with probability at least*

$$p_{succ} \geq p_\alpha(M)\left(\frac{1-\nu(n)}{d}\right) \tag{52}$$

where ν is exponentially small in n. Furthermore, assuming the protocol succeeds, if $n \geq \frac{32 \cdot 2^{4M}}{\delta^2 R \log_{2^{4M}} 2} = \frac{M 2^{4M+5}}{\delta^2 R}$ then the final state ρ' satisfies

$$F(|\alpha\rangle\langle\alpha|, \rho') \geq \left(1 - \sqrt{1 - p_\alpha(M)} - \delta\right)^2.$$

Proof The entanglement concentration of $|\Phi(r)\rangle$ and the encoding of $|\alpha\rangle$ are two procedures with independent success probabilities. Therefore, the overall probability of success is given by each of the two events being successful i.e. we multiply their respective probabilities of success according to Corollary 6.6 and Lemma 6.7 to obtain (52).

Let $\mathcal{T}$ be the action of Protocol 6.2. Note that (if successful), the output is $\rho' = \mathcal{D}_M \circ \mathcal{T} \circ \mathcal{E}_M(|\alpha\rangle\langle\alpha|)$. By the triangle inequality

$$D := \left\||\alpha\rangle\langle\alpha| - \mathcal{D}_M \circ \mathcal{T} \circ \mathcal{E}_M(|\alpha\rangle\langle\alpha|)\right\|_1 \leq D_1 + D_2 \qquad \text{where}$$

$$D_1 = \left\||\alpha\rangle\langle\alpha| - \mathcal{D}_M \circ \mathcal{E}_M(|\alpha\rangle\langle\alpha|)\right\|_1$$

$$D_2 = \left\|\mathcal{D}_M \circ \mathcal{E}_M(|\alpha\rangle\langle\alpha|) - \mathcal{D}_M \circ \mathcal{T} \circ \mathcal{E}_M(|\alpha\rangle\langle\alpha|)\right\|_1.$$

By Lemma 6.7, we have $D_1 \leq \sqrt{1 - p_\alpha(M)}$. Furthermore, by monotonicity, we have

$$D_2 \leq \|\mathcal{E}_M(|\alpha\rangle\langle\alpha|) - \mathcal{T} \circ \mathcal{E}_M(|\alpha\rangle\langle\alpha|)\|_1.$$

The latter is simply the distance $\|\rho - \mathcal{T}(\rho)\|_1$ between $\rho = \mathcal{E}_M(|\alpha\rangle\langle\alpha|)$ and its port-based teleported version $\mathcal{T}(\rho)$. Hence we can say that

$$D_2 = \|\mathcal{T}(\rho) - \rho\|_1 \leq \|\mathcal{T} - \mathbb{I}\|_\diamond \leq \delta \, , \tag{53}$$

where the first inequality comes from the definition of the diamond norm (6) and the second comes from Corollary 6.6 with $d = 2^M$. Therefore

$$\left\||\alpha\rangle\langle\alpha| - \rho'\right\|_1 \leq \sqrt{1 - p_\alpha(M)} + \delta$$

and by using (5), the claim follows. ∎

In fact, if sufficiently many copies of $|\Phi(r)\rangle$ are available, we can repeat again the entanglement concentration in Subprotocol 6.2 to make the failure probability of the entanglement concentration negligible. Theorem 6.8 shows that, at least in principle, port-based teleportation with continuous variable resources and states is possible if sufficiently many two-mode squeezed states are available.

7 Conclusions

In this thesis, we studied port-based teleportation for continuous variable systems. Focusing our efforts on Gaussian states and more specifically on coherent states and squeezed states, we have established that many results in the finite-dimensional case still hold for the infinite-dimensional case. Notably, we have proven that the fidelity of port-based teleportation for coherent states is

directly related to the probability of success of distinguishing an ensemble of states specified by the input and resources of port-based teleportation. Furthermore, we have explored the relationship between the average fidelity when teleporting coherent states distributed with a Gaussian prior and the entanglement fidelity of teleporting one mode of a two-mode squeezed state. This allowed us to state that the ability to teleport one mode of a two-mode squeezed state was a sufficient condition to be able to teleport a coherent state with Gaussian prior.

We also described a procedure for port-based teleportation with pre- and post-processing where the infinite-dimensional resources and coherent state input were converted to finite-dimensional systems so we could apply known protocols. We concluded that it is possible, in principle, to do port-based teleportation for continuous variable systems with a finite amount of resources. Furthermore, we presented port-based superdense coding, a superdense coding scheme inspired by port-based teleportation that allows us to enhance classical communication by using entanglement and quantum communication.

There are still many open questions to answer on the subject. We obtained a proof of principle for port-based teleportation of continuous variables by constructing a protocol with pre- and post-processing. Ideally, we would like to have a more direct procedure to teleport infinite-dimensional states by finding a measurement giving lower bounds on the fidelity of the process. Furthermore, our constructive protocol assumes a finite but large amount of entanglement. It would be useful to investigate what the minimal resources are (in terms of pure or impure entanglement), which are required to accomplish port-based teleportation. Ultimately, we would like to show that it is possible to implement port-based teleportation for continuous variable systems with linear quantum optics elements. This would provide a practical way of realizing the applications of port-based teleportation.

References

[1] NIELSEN, Michael A. and CHUANG, Isaac L. Quantum computation and quantum information. Cambridge university press, 2010.

[2] BRASSARD, Gilles and RAYMOND-ROBICHAUD, Paul. Can free will emerge from determinism in quantum theory?. In : *Is Science Compatible with Free Will?*. Springer New York, 2013. p. 41-61.

[3] STINESPRING, W. Forrest. Positive functions on C*-algebras. *Proceedings of the American Mathematical Society*, 1955, vol. 6, no 2, p. 211-216.

[4] PRESKILL, John. Lecture notes for physics 229: Quantum information and computation. *California Institute of Technology*, 1998.

[5] UHLMANN, Armin. The "transition probability" in the state space of a*-algebra. *Reports on Mathematical Physics*, 1976, vol. 9, no 2, p. 273-279.

[6] HELSTROM, Carl Wilhelm. *Quantum detection and estimation theory*. Academic press, 1976.

[7] HAUSLADEN, Paul and WOOTTERS, William K. A 'pretty good'measurement for distinguishing quantum states. *Journal of Modern Optics*, 1994, vol. 41, no 12, p. 2385-2390.

[8] BARNUM, H. and KNILL, E. Reversing quantum dynamics with near-optimal quantum and classical fidelity. *Journal of Mathematical Physics*, 2002, vol. 43, no 5, p. 2097-2106.

[9] YUEN, Horace PH. Communication theory of quantum systems. 1971. *Doctoral dissertation* Massachusetts inst of tech Cambridge research lab of electronics.

[10] BENNETT, Charles H., BRASSARD, Gilles, et al. Quantum cryptography: Public key distribution and coin tossing. In : *Proceedings of IEEE International Conference on Computers, Systems and Signal Processing*. 1984.

[11] BENNETT, Charles H., BRASSARD, Gilles, CRÉPEAU, Claude, et al. Teleporting an unknown quantum state via dual classical and Einstein-Podolsky-Rosen channels. *Physical Review Letters*, 1993, vol. 70, no 13, p. 1895.

[12] SHOR, Peter W. Algorithms for quantum computation: discrete logarithms and factoring. In : *Foundations of Computer Science, 1994 Proceedings., 35th Annual Symposium on.* IEEE, 1994. p. 124-134.

[13] ADESSO, Gerardo, RAGY, Sammy, and LEE, Antony R. Continuous variable quantum information: Gaussian states and beyond. *Open Systems and Information Dynamics*, 2014, vol. 21, no 01n02.

[14] BRAUNSTEIN, Samuel L. Squeezing as an irreducible resource. *Physical Review A*, 2005, vol. 71, no 5, p. 055801.

[15] DE GOSSON, Maurice A. *Symplectic geometry and quantum mechanics*. Springer, 2006.

[16] HORODECKI, Michał, HORODECKI, Paweł, and HORODECKI, Ryszard. General teleportation channel, singlet fraction, and quasidistillation. *Physical Review A*, 1999, vol. 60, no 3, p. 1888.

[17] BEIGI, Salman and KÖNIG, Robert. Simplified instantaneous non-local quantum computation with applications to position-based cryptography. *New Journal of Physics*, 2011, vol. 13, no 9, p. 093036.

[18] ISHIZAKA, Satoshi and HIROSHIMA, Tohya. Quantum teleportation scheme by selecting one of multiple output ports. *Physical Review A*, 2009, vol. 79, no 4, p. 042306.

[19] ISHIZAKA, Satoshi and HIROSHIMA, Tohya. Asymptotic teleportation scheme as a universal programmable quantum processor. *Physical Review Letters*, 2008, vol. 101, no 24, p. 240501.

[20] KOGIAS, Ioannis, RAGY, Sammy, and ADESSO, Gerardo. Continuous-variable versus hybrid schemes for quantum teleportation of Gaussian states. *Physical Review A*, 2014, vol. 89, no 5, p. 052324.

[21] MATSUMOTO, Keiji and HAYASHI, Masahito. Universal distortion-free entanglement concentration. *Physical Review A*, 2007, vol. 75, no 6, p. 062338.

[22] MATSUMOTO, Keiji. Self-teleportation and its application on LOCC estimation and other tasks. *arXiv preprint arXiv:0709.3250*, 2007.

[23] CHIRIBELLA, Giulio and XIE, Jinyu. Optimal design and quantum benchmarks for coherent state amplifiers. *Physical Review Letters*, 2013, vol. 110, no 21, p. 213602.

[24] WERNER, Reinhard F. All teleportation and dense coding schemes. *Journal of Physics A: Mathematical and General*, 2001, vol. 34, no 35, p. 7081.

[25] VAIDMAN, Lev. Teleportation of quantum states. *Physical Review A*, 1994, vol. 49, no 2, p. 1473.

[26] BRAUNSTEIN, Samuel L. and KIMBLE, H. Jeff. Teleportation of continuous quantum variables. *Physical Review Letters*, 1998, vol. 80, no 4, p. 869.

[27] TAN, Si Hui, et al. Quantum state discrimination with bosonic channels and gaussian states. 2010. *Doctoral dissertation.* Massachusetts Institute of Technology.

[28] SANCHEZ, R. García-Patrón. Quantum Information with Optical Continuous Variables: from Bell Tests to Key Distribution. 2007. *Doctoral dissertation.* Université Libre de Bruxelles.

[29] KRÜGER, Ole. Quantum information theory with Gaussian systems. 2006. *Doctoral dissertation.* Technische Universität Carolo-Wilhelmina zu Braunschweig.

[30] EISERT, Jens and WOLF, Michael M. Gaussian quantum channels. *arXiv preprint* quant-ph/0505151, 2005.

[31] VAIDMAN, Lev. Instantaneous measurement of nonlocal variables. *Physical Review Letters*, 2003, vol. 90, no 1, p. 010402.

[32] NAMIKI, Ryo. Fundamental quantum limits on phase-insensitive linear amplification and phase conjugation in a practical framework. *Physical Review A*, 2011, vol. 83, no 4, p. 040302.

[33] ANDERSEN, Ulrik L. et RALPH, Timothy C. High-fidelity teleportation of continuous-variable quantum states using delocalized single photons. *Physical review letters*, 2013, vol. 111, no 5, p. 050504.

A   Proof of Lemma 3.3

In this section, we provide the proof to Lemma 3.3 presented in section 3.4.4.

Proof The characteristic function reads

$$
\begin{aligned}
\chi_{\tilde{\rho}_A}(\xi) &= \mathsf{tr}(\tilde{\rho}_A D(\xi)) \\
&= \frac{1}{p(\psi)}\mathsf{tr}((D(\xi) \otimes |\psi\rangle\langle\psi|)\rho_{AB}) \\
&= \frac{1}{(2\pi)^{n_B}p(\psi)} \int \chi_{|\psi\rangle\langle\psi|}(-\eta)\mathsf{tr}\left((D(\xi) \otimes D(\eta))\rho_{AB}\right) d^2\eta \\
&= \frac{1}{(2\pi)^{n_B}p(\psi)} \int \chi_{|\psi\rangle\langle\psi|}(-\eta)\chi_{\rho_{AB}}(\xi,\eta)d^2\eta \; ,
\end{aligned}
$$

hence (26) follows. Using (27) and the block-diagonal form

$$
\sigma_{AB} = \begin{pmatrix} \sigma_A & 0 \\ 0 & \sigma_B \end{pmatrix} \; ,
$$

90

yields

$$\chi_{\rho_{AB}}(\xi, \eta) = \exp\left(-\frac{1}{4}\xi^T \sigma_A^T \gamma_A \sigma_A \xi - \frac{1}{4}\eta^T \sigma_B^T \gamma_B \sigma_B \eta - \frac{1}{2}\xi^T \sigma_A^T \delta_{AB}\sigma_B\eta - id_A^T\sigma_A\xi - id_B^T\sigma_B\eta\right)$$

$$= \exp\left(-\frac{1}{4}(\sigma_A\xi)^T \gamma_A \sigma_A \xi - \frac{1}{4}(\sigma_B\eta)^T \gamma_B \sigma_B \eta - \frac{1}{2}(\sigma_A\xi)^T \delta_{AB}\sigma_B\eta - id_A^T\sigma_A\xi - id_B^T\sigma_B\eta\right)$$

By definition (22), the characteristic function is expressed as

$$\chi_{|\psi\rangle\langle\psi|}(\eta) = \exp\left(-\frac{1}{4}(\sigma_B\eta)^T \gamma_\psi \sigma_B \eta - id_\psi^T\sigma_B\eta\right)$$

Inserting the last two expressions into (26) gives

$$(2\pi)^{n_B}p(\psi)\chi_{\tilde{\rho}_A}(\xi) = \exp\left(-\frac{1}{4}(\sigma_A\xi)^T \gamma_A \sigma_A \xi - id_A^T\sigma_A\xi\right) \cdot I \qquad \text{where}$$

$$I := \int \exp\left(-\frac{1}{4}(\sigma_B\eta)^T(\gamma_B + \gamma_\psi)\sigma_B\eta - \frac{1}{2}(\sigma_A\xi)^T\delta_{AB}\sigma_B\eta - i(d_B - d_\psi)^T\sigma_B\eta\right)d^2\eta$$

Substituting $\eta \to \sigma_B\eta$, and applying $\int \exp\left(-\frac{1}{2}x^T Ax + B^Tx\right)dx = \sqrt{\frac{(2\pi)^n}{\det A}}\exp(\frac{1}{2}B^T A^{-1}B)$ to

$$A = (\gamma_B + \gamma_\psi)/2 \qquad \text{and} \qquad B = -\frac{1}{2}\delta_{AB}^T\sigma_A\xi - i(d_B - d_\psi)$$

gives

$$(2\pi)^{n_B}p(\psi)\chi_{\tilde{\rho}_{AB}}(\xi) = c \cdot \exp\left(\frac{1}{4}\xi^T\sigma_A^T\delta_{AB}(\gamma_A + \gamma_\psi)^{-1}\delta_{AB}^T\sigma_A\xi + i\xi^T\sigma_A^T\delta_{AB}(\gamma_B + \gamma_\psi)^{-1}(d_B - d_\psi)\right).$$

Since

$$c = \frac{1}{\sqrt{(\gamma_A + \gamma_\psi)/2}}\exp\left(-\frac{1}{4}(\sigma_A\xi)^T\gamma_A\sigma_A\xi - id_A^T\sigma_A\xi - (d_B - d_\psi)^T(\gamma_B + \overline{\gamma})_B^{-1}(d_B - d_\psi)\right)$$

91

it is possible to separate the quadratic, linear and constant part in ξ

$$(2\pi)^{n_B} p(\psi) \chi_{\tilde{\rho}_{AB}}(\xi) = I_{quad} \cdot I_{lin} \cdot I_{const}$$

where

$$I_{quad} = \exp\left(-\frac{1}{4}(\sigma_A \xi)^T [\gamma_A - \delta_{AB}(\gamma_A + \gamma_\psi)^{-1} \delta_{AB}^T](\sigma_A \xi)\right)$$

$$I_{lin} = \exp\left(-i[d_A + \delta_{AB}(\gamma_B + \gamma_\psi)^{-1}(d_\psi - d_B)]^T (\sigma_A \xi)\right)$$

$$I_{const} = \exp\left(-(d_B - d_\psi)^T (\gamma_B + \gamma_\psi)^{-1}(d_B - d_\psi)\right).$$

From the linear and quadratic term along with the definition for the characteristic function (22) it is easy to compare and identify $\tilde{\gamma}$ and $\tilde{d}_A$ as introduced in the statement of the lemma. Furthermore, the term that is independent of ξ can be associated with the normalized probability distribution $p(\psi)$. ∎

B   Proof of Lemma 3.4

In this section, we present the proof of 3.4 presented in section 3.4.4.

Proof Observe that the POVM element associated with m corresponds to projecting the B system onto a Gaussian state with covariance matrix γ_ψ and displacement m; hence this corresponds to the situation of Lemma 3.3. The measurement E_m on system B and the displacement $D(\Gamma m)$ on system A commute. Therefore we can rewrite (29) as

$$\mathcal{E}(\rho_{AB}) = \int \text{tr}_B((\mathbb{1}_A \otimes E_B^m)\rho_{AB}^{\Gamma m}) d^{2n_B} m \tag{54}$$

where

$$\rho_{AB}^{\Gamma m} = (D(\Gamma m) \otimes \mathbb{1}_B)\rho_{AB}(D(\Gamma m)^\dagger \otimes \mathbb{1}_B).$$

Notice that $\rho_{AB}^{\Gamma m}$ has the same covariance matrix as ρ_{AB}, and displacement

$$d_A^{\Gamma m} = d_A + \Gamma m$$

$$d_B^{\Gamma m} = d_B.$$

whereas $D(m)|\psi\rangle$ has displacement d_B. Therefore Lemma 3.3 tells us

$$\text{tr}((D(\xi) \otimes E_B^m)\rho_{AB}^{\Gamma m}) = I_{quad} \cdot I_{lin}(m) \cdot p(m) \ ,$$

where

$$I_{quad} = \exp\left(-\frac{1}{4}(\sigma_A\xi)^T[\gamma_A - \delta_{AB}(\gamma_A + \gamma_\psi)^{-1}\delta_{AB}^T](\sigma_A\xi)\right)$$

$$I_{lin}(m) = \exp\left(-i[d_A + \Gamma m + \delta_{AB}(\gamma_B + \gamma_\psi)^{-1}(m - d_B)]^T(\sigma_A\xi)\right)$$

$$p(m) = \frac{1}{\pi^{n_B}\sqrt{\det(\gamma_B + \gamma_\psi)}} \exp\left(-(m - d_B)^T(\gamma_B + \gamma_\psi)^{-1}(m - d_B)\right).$$

With (54) and linearity, this implies

$$\text{tr}(\mathcal{E}(\rho_{AB})D(\xi)) = I_{quad}\int I_{lin}(m)p(m)d^{2n_B}m$$

$$= I_{quad}\exp(-i(d_A + \Gamma d_B)^T\sigma_A\xi)I \tag{55}$$

where, using the substitution $m = m - d_B$, I is the integral

$$I = \frac{1}{\pi^{n_B} \sqrt{\det(\gamma_B + \gamma_\psi)}} \int \exp\left(-m^T(\gamma_B + \gamma_\psi)^{-1}m - i(\sigma_A\xi)^T[\Gamma + \delta_{AB}(\gamma_B + \gamma_\psi)^{-1}]m\right) d^{2n_B}m$$

$$= \exp\left(-\frac{1}{4}(\sigma_A\xi)^T[\Gamma + \delta_{AB}(\gamma_B + \gamma_\psi)^{-1}](\gamma_B + \gamma_\psi)[\Gamma + \delta_{AB}(\gamma_B + \gamma_\psi)^{-1}]^T(\sigma_A\xi)\right).$$

Combining with the quadratic terms in ξ from (55) and using the fact that covariance matrices are symmetric ($\gamma^T = \gamma$), we see that $\mathcal{E}(\rho_{AB})$ has a characteristic function

$$\chi_{\mathcal{E}(\rho_{AB})} = \exp\left(-\frac{1}{4}(\sigma_A\xi)^T\left[\gamma_A + \Gamma(\gamma_B + \gamma_\psi)\Gamma^T + \Gamma\delta_{AB}^T + \delta_{AB}\Gamma^T\right](\sigma_A\xi) - i(d_A + \Gamma d_B)^T(\sigma_A\xi)\right)$$

which matches the statement of the lemma. ∎

C Characteristic function for the teleportation of arbitrary input state

All the steps involved in the calculation of Section 4.2.3 are reconsidered in terms of their effect on the characteristic function of the states. Our results are summarized in the following lemma which analyses the effect of Protocol 4.2.

Lemma C.1 (Homodyne measurement for imperfect squeezing) *Assume Alice has the state* ρ_{in} *specified as mode 3 (with covariance matrix* $\gamma_{in} = \begin{pmatrix} a & b \\ c & d \end{pmatrix}$ *and displacement* d_{in}*) to teleport and mode 2 from the two-mode squeezed state* $\rho_{12} = |\Phi(r)\rangle_{12}$ *(which means Bob has mode 1). After the application of Protocol 4.2 by Alice and Bob, Bob will have in his possession a quantum state*

that has a characteristic function described by the covariance matrix

$$\gamma_{out} = \begin{pmatrix} \frac{a+2d+\cosh(2r)(2-2c^2+2ad)+a\cosh(4r)}{1-2c^2+2ad+2\cosh(2r)(a+d)+\cosh(4r)} & \frac{c\sinh^2(2r)}{-c^2+ad+\cosh(2r)(a+d)+\cosh^2(2r)} \\ \frac{2c\sinh^2(2r)}{-c^2+ad+\cosh(2r)(a+d)+\cosh^2(2r)} & \cosh(2r) - \frac{(a+\cosh(2r))\sinh^2(2r)}{-c^2+ad+\cosh(2r)(a+d)+\cosh^2(2r)} \end{pmatrix} \tag{56}$$

and displacement

$$d_{out} = \begin{pmatrix} -\frac{\sqrt{2}\sinh(2r)(\sqrt{2}cp-2cp_\psi-\sqrt{2}dx+2dx_\psi+\cosh(2r)(2x_\psi-\sqrt{2}x))}{1-2c^2+2ad+2\cosh(2r)(a+d)+\cosh(4r)} \\ \frac{\sqrt{2}\sinh(2r)(\sqrt{2}ap-2ap_\psi-\sqrt{2}cx+2cx_\psi+\cosh(2r)(2p_\psi-\sqrt{2}p))}{1-2c^2+2ad+2\cosh(2r)(a+d)+\cosh(4r)} \end{pmatrix}. \tag{57}$$

where x_ψ and p_ψ are the results from the homodyne measurements. In particular, in the limit $r \to \infty$, we recover γ_{in} and $d_{in} - \sqrt{2}(x_\psi, p_\psi)^T$. Furthermore, the covariance matrix γ_{av} and displacement d_{av} averaged over the measurement outcomes for the homodyne measurement are given by

$$\gamma_{av} = \begin{pmatrix} a + 2\cosh(2r) - 2\sinh(2r) & b \\ c & d + 2\cosh(2r) - 2\sinh(2r) \end{pmatrix} \tag{58}$$

and

$$d_{av} = (x,p)^T \tag{59}$$

which both reduce to the initial input when $r \to \infty$.

Proof The initial state of the system is $\rho = \rho_{12} \otimes \rho_{in}$ with characteristic function $\chi(\xi_1, \xi_2, \xi_3)$. In step 1, Alice applies a 50:50 beam-splitter (25) on her two modes, $\rho' = (\mathbb{1}_2 \otimes U)\rho(\mathbb{1}_2 \otimes U^\dagger)$. As mentioned in Theorem 3.1, the effect on the quadratures are reflected in the following modification

95

for the characteristic function

$$\chi' = \chi(\xi_1, \frac{1}{\sqrt{2}}\xi_2 - \frac{1}{\sqrt{2}}\xi_3, \frac{1}{\sqrt{2}}\xi_2 + \frac{1}{\sqrt{2}}\xi_3)$$
$$= \chi(S\vec{\xi})$$

where

$$S = \begin{pmatrix} \mathbb{1} & 0 & 0 \\ 0 & \frac{\mathbb{1}}{\sqrt{2}} & -\frac{\mathbb{1}}{\sqrt{2}} \\ 0 & \frac{\mathbb{1}}{\sqrt{2}} & \frac{\mathbb{1}}{\sqrt{2}} \end{pmatrix}.$$

These transformation can be restated on the covariance matrix level. Indeed, the covariance matrix of the initial system is $\gamma_{12} \oplus \gamma_\psi$ and the displacement is $(\vec{0}, d_\psi)^T$. The characteristic function after applying the beam-splitter can then be written

$$\chi(S\vec{\xi}) = \exp\left\{ -\frac{1}{4}\xi^T S^T \sigma^T (\gamma_{12} \oplus \gamma_\rho)\sigma S\xi - i(\vec{0}, d_\rho)\sigma S\xi \right\}.$$

Since S and σ commute, the transformation can be interpreted as

$$\gamma \to S^T \gamma S \qquad \text{and} \qquad d \to S^T d.$$

Step 2 in the protocol is the homodyne measurement. The measurement of the p quadrature on the third mode and x on the second mode can be analysed using Lemma 3.3. Therefore all the calculations can be done directly on the level of the covariance matrix and the displacement.

Let us proceed step by step. The initial covariance matrix of $\rho_{12} \otimes \rho_{in}$ is given by the direct sum

$$\gamma = \gamma_{12} \oplus \gamma_{in}$$

and because γ_{12} is a two-mode squeezed state,

$$\gamma = \begin{pmatrix} \cosh(2r)\mathbb{1} & \sinh(2r)\sigma_z & 0 \\ \sinh(2r)\sigma_z & \cosh(2r)\mathbb{1} & 0 \\ 0 & 0 & \gamma_{in} \end{pmatrix}.$$

Step 1 is the application of the beam-splitter which results in the covariance matrix

$$S^T\gamma S = \begin{pmatrix} \cosh(2r)\mathbb{1} & \frac{1}{\sqrt{2}}\sinh(2r)\sigma_z & -\frac{1}{\sqrt{2}}\sinh(2r)\sigma_z \\ \frac{1}{\sqrt{2}}\sinh(2r)\sigma_z & \frac{1}{2}(\cosh(2r)\mathbb{1} + \gamma_{in}) & -\frac{1}{2}(\cosh(2r)\mathbb{1} - \gamma_{in}) \\ -\frac{1}{\sqrt{2}}\sinh(2r)\sigma_z & -\frac{1}{2}(\cosh(2r)\mathbb{1} - \gamma_{in}) & \frac{1}{2}(\cosh(2r)\mathbb{1} + \gamma_{in}) \end{pmatrix}.$$

Step 2 begins with the measurement of the x quadrature on the third mode. Using Lemma 3.3 with

$$\gamma_A = \begin{pmatrix} \cosh(2r)\mathbb{1} & \frac{1}{\sqrt{2}}\sinh(2r)\sigma_z \\ \frac{1}{\sqrt{2}}\sinh(2r)\sigma_z & \frac{1}{2}(\cosh(2r)\mathbb{1} + \gamma_{in}), \end{pmatrix} \qquad \text{and} \qquad \gamma_B = \frac{1}{2}(\cosh(2r)\mathbb{1} + \gamma_{in})$$

$$\delta_{AB} = \begin{pmatrix} -\frac{1}{\sqrt{2}}\sinh(2r)\sigma_z \\ -\frac{1}{2}(\cosh(2r)\mathbb{1} - \gamma_{in}) \end{pmatrix}$$

for the formula

$$\tilde{\gamma} = \gamma_A - \delta_{AB}(\gamma_B + \gamma_\psi)^{-1}\delta_{AB}^T.$$

We have already covered this case in Section 3.4.5 and know the inverse matrix is just the inverse

of the first entry of γ_B and 0 everywhere else. The new covariance matrix then reads

$$\tilde{\gamma} = \begin{pmatrix} \cosh(2r) - \frac{\sinh^2(2r)}{\cosh(2r)+a} & 0 & \sinh(2r)\frac{1}{\sqrt{2}}\left(1 + \frac{a-\cosh(2r)}{a+\cosh(2r)}\right) & \frac{1}{\sqrt{2}}\frac{\sinh(2r)c}{\cosh(2r)+a} \\ 0 & \cosh(2r) & 0 & -\frac{1}{\sqrt{2}}\sinh(2r) \\ \sinh(2r)\frac{1}{\sqrt{2}}\left(1 + \frac{a-\cosh(2r)}{a+\cosh(2r)}\right) & 0 & \frac{1}{2}(\cosh(2r)+a)\left(\frac{(a-\cosh(2r))^2}{2a+2\cosh(2r)}\right) & \frac{1}{2}\left(b - \frac{ac-c\cosh(2r)}{a+\cosh(2r)}\right) \\ \frac{1}{\sqrt{2}}\frac{\sinh(2r)c}{\cosh(2r)+a} & -\frac{1}{\sqrt{2}}\sinh(2r) & \frac{1}{2}\left(b - \frac{ac-c\cosh(2r)}{a+\cosh(2r)}\right)c & \frac{1}{2}(\cosh(2r)+d) - \frac{c^2}{2(\cosh(2r)+a)} \end{pmatrix}$$

We proceed similarly to analyse the measurement of the p quadrature. Again, we use the results of Lemma 3.3 with

$$\gamma_A = \begin{pmatrix} \cosh(2r) - \frac{\sinh^2(2r)}{\cosh(2r)+a} & 0 \\ 0 & \cosh(2r) \end{pmatrix}$$

$$\gamma_B = \begin{pmatrix} \frac{1}{2}(\cosh(2r)+a)\left(\frac{(a-\cosh(2r))^2}{2a+2\cosh(2r)}\right) & \frac{1}{2}\left(b - \frac{ac-c\cosh(2r)}{a+\cosh(2r)}\right) \\ \frac{1}{2}\left(b - \frac{ac-c\cosh(2r)}{a+\cosh(2r)}\right)c & \frac{1}{2}(\cosh(2r)+d) - \frac{c^2}{2(\cosh(2r)+a)} \end{pmatrix}$$

$$\delta_{AB} = \begin{pmatrix} \sinh(2r)\frac{1}{\sqrt{2}}\left(1 + \frac{a-\cosh(2r)}{a+\cosh(2r)}\right) & \frac{1}{\sqrt{2}}\frac{\sinh(2r)c}{\cosh(2r)+a} \\ 0 & -\frac{1}{\sqrt{2}}\sinh(2r) \end{pmatrix}$$

and the formula

$$\tilde{\gamma} = \gamma_A - \delta_{AB}(\gamma_B + \gamma_\psi)^{-1}\delta_{AB}^T.$$

This gives the claim form of the final covariance matrix γ_{out} (56).

The analysis of the displacement proceeds in a similar fashion. The initial displacement of the state to teleport being $d_{in} = (x, p)$

$$d = S^T \otimes \mathbb{1}(0, 0, d_{in})^T$$
$$= \frac{1}{\sqrt{2}}(0, 0, x, p, x, p)^T.$$

The transformation due to the measurement of the x quadrature on the last mode is given by Lemma 3.3

$$\tilde{d}_A = d_A + \delta_{AB}(\gamma_B + \gamma_\psi)^{-1}(d_\psi - d_B)$$

where

$$d_A = \frac{1}{\sqrt{2}}(0, 0, x, p)^T, \qquad d_B = \frac{1}{\sqrt{2}}(x, p)^T \qquad \text{and} \qquad d_\psi = (x_\psi, 0)^T$$

and therefore

$$\tilde{d} = \frac{1}{\cosh(2r) + a}\begin{pmatrix} (\sqrt{2}x_\psi - x)\sinh(2r) \\ 0 \\ \frac{x}{\sqrt{2}}(a + \cosh(2r)) + (x_\psi - \frac{x}{\sqrt{2}})(a - \cosh(2r)) \\ \frac{p}{\sqrt{2}}(a + \cosh(2r)) + c\left(x_\psi - \frac{x}{\sqrt{2}}\right) \end{pmatrix}.$$

Using the formula once again but this time with $d_\psi = (0, p_\psi)^T$ to analyse the p-quadrature measurement, we get the displacement of the output state (57).

If we want the expression for the covariance matrix and the displacement averaged on the measurement outcome after Bob has done the displacement to complete the protocol, then we can use 3.4. Using

$$\Gamma = \begin{pmatrix} 0 & 0 & \sqrt{2} & 0 \\ 0 & \sqrt{2} & 0 & 0 \end{pmatrix}, \qquad \gamma_A = \cosh(2r)\mathbb{1},$$

$$\gamma_B = \begin{pmatrix} \frac{1}{2}(\cosh(2r)\mathbb{1} + \gamma_{in}) & -\frac{1}{2}(\cosh(2r)\mathbb{1} - \gamma_{in}) \\ -\frac{1}{2}(\cosh(2r)\mathbb{1} - \gamma_{in}) & \frac{1}{2}(\cosh(2r)\mathbb{1} + \gamma_{in}) \end{pmatrix},$$

$$\delta_{AB} = \left(\frac{1}{\sqrt{2}} \sinh(2r)\sigma_z \quad -\frac{1}{\sqrt{2}} \sinh(2r)\sigma_z \right)$$

and

$$d_A = (0,0)^T \qquad \text{and} \qquad d_B = \frac{1}{\sqrt{2}}(x, p, x, p)$$

with the formulas

$$\tilde{\gamma}_A = \gamma_A + \Gamma(\gamma_B + \gamma_\psi)\Gamma^T + \Gamma\delta_{AB}^T + \delta_{AB}\Gamma^T$$
$$\tilde{d}_A = d_A + \Gamma d_B.$$

to obtain equation (58) and (59). In that case, we used

$$\gamma_\psi = \begin{pmatrix} e^{-r1} & 0 & 0 & 0 \\ 0 & e^{-r1} & 0 & 0 \\ 0 & 0 & e^{-r2} & 0 \\ 0 & 0 & 0 & e^{-r2} \end{pmatrix}$$

with the limit $r_1, r_2 \to \infty$. This concludes the proof. ∎

Note that by taking $a = d = 1, b = c = 0$ we obtain that the average covariance is given by

$$\gamma_{av} = (1 + 2e^{-2r})\mathbb{1} \tag{60}$$

i.e. the averaged output of the teleportation is a thermal state.

D   Fidelity formula for two Gaussian states when one of them is pure

In this appendix, we attempt to obtain a formula for the fidelity of two Gaussian states in the special case where one of them is pure, say the two states are ρ (covariance matrix γ_ρ and displacement d_ρ) and $|\psi\rangle$ (covariance matrix γ_ψ and displacement d_ψ). We use this assumption because the fidelity of two quantum states is quite simpler if one of the states is pure

$$F = \mathsf{tr}(|\psi\rangle\langle\psi|\rho).$$

Using this formula along with the decomposition of any quantum state into displacement operators (21) gives us

$$F = \mathsf{tr}\left(|\psi\rangle\langle\psi|\frac{1}{(2\pi)^N}\int d^{2N}\xi\chi_\rho(-\xi)D_\xi\right)$$

and since the trace is linear,

$$F = \frac{1}{(2\pi)^N}\int d^{2N}\xi\chi_\rho(-\xi)\mathsf{tr}\left(|\psi\rangle\langle\psi|D_\xi\right)$$

and we recognize the definition for the characteristic function

$$F = \frac{1}{(2\pi)^N}\int d^{2N}\xi\chi_\rho(-\xi)\chi_\psi(\xi).$$

Assuming the two quantum states are Gaussian states we can exploit the formula for their characteristic functions (22)

$$F = \frac{1}{(2\pi)^N} \int d^{2N}\xi \exp(-\frac{1}{4}\xi^T \sigma^T (\gamma_\rho + \gamma_\psi)\sigma\xi - i(d_\rho - d_\psi)^T \sigma\xi)$$

we can make the substitution $\xi \to \sigma\xi$ (the Jacobian is 1) and carry out the Gaussian integral to obtain

$$F = \frac{2\exp\left(-(d_\rho - d_\psi)^T (\gamma_\rho + \gamma_\psi)^{-1}(d_\rho - d_\psi)\right)}{\sqrt{\det(\gamma_\rho + \gamma_\psi)}}. \tag{61}$$

This formula is used to obtain equation (34).

E Lower bound for PGM

Here we explicitly carry the calculations in Section 5.3 to obtain equation (39). We use the bound on the probability of success of the PGM [17]

$$p_{succ}^{PGM} \geq \frac{1}{N\bar{r}\mathrm{tr}\bar{\rho}^2}$$

where $\bar{r} = \frac{1}{N}\sum_i \mathrm{rank}(\rho_i)$ is the average rank and in the same fashion $\bar{\rho} = \frac{1}{N}\sum_i \rho_i$ is the average of the states to distinguish.

For the present problem, the average rank is given by d^{N-1} (each maximally mixed state has rank d and the maximally entangled state occupies two ports and is of rank 1). We also have

$$\mathrm{tr}(\bar{\rho}^2) = \frac{1}{N^2}\sum_{ij}\mathrm{tr}(\rho_i\rho_j) = \frac{1}{N^2}\left(N\mathrm{tr}(\rho_i^2) + (N^2 - N)\mathrm{tr}(\rho_i\rho_j)\right) = \frac{1}{Nd^{N-1}} + \frac{N-1}{Nd^{N+1}}.$$

Therefore we need to compute both $\mathsf{tr}(\rho_i^2)$ and $\mathsf{tr}\rho_i\rho_j$. First we have

$$\mathsf{tr}(\rho_i^2) = \mathsf{tr}\left(\Phi_{SA_i} \otimes (\mathbb{1}/d^2)_{\bar{A}_i}^{\otimes(N-1)}\right) = \frac{1}{d^{N-1}}.$$

and

$$\mathsf{tr}\rho_i\rho_j = \frac{1}{d^N}\mathsf{tr}\left[\left(\Phi_{SA_i} \otimes \mathbb{1}_{A_j}\right)\left(\Phi_{SA_j} \otimes \mathbb{1}_{A_i}\right)\right].$$

For this last expresion, it is simpler to start with

$$
\begin{aligned}
(\langle\Phi|_{SA_i} \otimes \mathbb{1}_{A_j})(|\Phi\rangle_{SA_j} \otimes \mathbb{1}_{A_i}) &= \frac{1}{d}\sum_{nm}(\langle n|_S\langle n|_{A_i} \otimes \mathbb{1}_{A_j})(|m\rangle_S|m\rangle_{A_j} \otimes \mathbb{1}_{A_i}) \\
&= \frac{1}{d}\sum_{n}|n\rangle_{A_j}\langle n|_{A_i}
\end{aligned}
$$

to notice that

$$\left(\Phi_{SA_i} \otimes \mathbb{1}_{A_j}\right)\left(\Phi_{SA_j} \otimes \mathbb{1}_{A_i}\right) = \frac{1}{d^2}\sum_{n}|n\rangle\langle n|_{A_i}$$

and therefore

$$\mathsf{tr}\rho_i\rho_j = \frac{1}{d^{N+1}}$$

so we can conclude

$$\mathsf{tr}(\bar{\rho}^2) = \frac{1}{N^2}\sum_{ij}\mathsf{tr}(\rho_i\rho_j) = \frac{1}{Nd^{N-1}} + \frac{N-1}{Nd^{N+1}}.$$

The bound is then found to be

$$p_{succ}^{PGM} \geq \frac{1}{Nd^{N-1}}\frac{Nd^{N+1}}{d^2+N-1} = \frac{d^2}{d^2+N-1} \tag{62}$$

and the related fidelity is

$$F_{ent} \geq \frac{N}{d^2}p_{succ}^{PGM} \geq \frac{N}{d^2+N-1}.$$

For N large enough, we can use the identity $(1+x)^n \approx 1+nx$ with $n = -1$

$$F_{ent} \geq 1 - \frac{d^2-1}{N}$$

which gives us equation (39).